Thallium isotopes as tracers of recycled materials in subduction zones: review and new data for lavas from Tonga-Kermadec and Central America

Sune G. Nielsen[1,2], Julie Prytulak[3], Jerzy Blusztajn[1,2], Yunchao Shu[1,2,4,5], Maureen Auro[1,2], Marcel Regelous[6] and Jim Walker[7]

[1]NIRVANA Laboratories, Woods Hole Oceanographic Institution, Woods Hole, MA, USA

[2]Department of Geology and Geophysics, Woods Hole Oceanographic Institution, Woods Hole, MA, USA

[3]Department of Earth Science and Engineering, Imperial College London, UK

[4]Institute of Oceanology, Chinese Academy of Sciences, Qingdao, China

[5]University of Chinese Academy of Sciences, Beijing, China

[6]GeoZentrum Nordbayern, Friedrich-Alexander-Universität Erlangen-Nürnberg, Erlangen, Germany

[7]Department of Geology and Environmental Geosciences, Northern Illinois University, DeKalb, IL, USA

Abstract - Sediment is actively being subducted in every convergent margin worldwide. Yet, geochemical data for arc lavas from several subduction zones, such as Northern Tonga and Costa Rica have revealed either attenuated or limited evidence for sediment in their mantle source regions. Here we use thallium (Tl) isotopes to trace slab components in lavas from the Tonga-Kermadec and Central American arcs. In general, both arcs display Tl isotope data that are most compatible with addition of sediment to the sub-arc mantle from the subducting slab. This evidence is particular strong in the Tonga-Kermadec arc where pelagic clays dominate the Tl budget along the entire arc. Contributions from altered oceanic crust as well as the Louisville Seamount chain that subducts underneath Northern Tonga are not visible in Tl isotopes, which is likely due to the very high Tl concentrations found in pelagic sediments outboard of the Tonga-Kermadec arc. Lavas from Central America reveal variable and systematic Tl isotope compositions along-strike. In particular, lavas from Nicaragua are dominated by contributions from sediments, whereas Costa Rican samples reveal a significant altered oceanic crust component with little influence from sediments on thallium isotope composition. The absence of a sediment signature in Costa Rica corresponds with the Cocos Ridge and the seamount province subduction, which results in a thinner sediment cover. Furthermore, the subducted sediment is dominated by carbonates with very low Tl concentrations and, therefore, small amounts of carbonate sediment added to the mantle wedge does not contribute significantly to the overall Tl budget.

A review of Tl isotope and concentration data from the Aleutians, Marianas, Tonga-Kermadec and Central American arcs demonstrate that pelagic sediments are detectable in most arcs , whereas altered oceanic crust components only become appreciable when sediment Tl concentrations are very low (e.g. carbonate) or if sediments are no longer a significant

component of the subducting slab (e.g. slab melting in Western Aleutians). As such, Tl isotopes is a promising tool to trace sediment subduction although this requires at least some pelagic sediment is present is the subducted sediment package.

We suggest that thallium partitioning between the slab and mantle wedge is most likely controlled by retention in phengite or by partitioning into fluids. Residual phengite likely produces high Cs/Tl ratios because Tl should be more compatible in phengite than is Cs, however, this conclusion needs experimental verification. The stability of phengite is lower at higher fluid contents, which results in hyperbolic relationships between Cs/Tl and possible indicators of fluids such as Sr/Nd and Ba/Th. Thus, combined Tl isotopic and and elemental systematics not only provide detailed information about the specific slab components that contribute to arc lavas, but also potentially shed light on the mineralogy and physical conditions of subducting slabs.

1. Introduction

It is well established that material released from subducting slabs imparts distinct chemical signatures to arc volcanism. Many lines of evidence suggest that both subducted sediments and hydrothermally altered ocean crust (AOC) can play significant roles in the chemistry of arc lavas (e.g. Elliott et al., 1997; Kay et al., 1978; Plank and Langmuir, 1993). However, even though sediment appears to be almost ubiquitously part of the subducted package (Plank and Langmuir, 1998) there are several arcs (or segments of arcs) that display very weak or debatably absent sediment signatures (Hawkesworth et al., 1997; Leeman et al., 2005; Morris et al., 1990; Regelous et al., 1997; Tera et al., 1986). The reasons for the attenuated sediment signatures in certain arcs are not clear and, in addition to the case of a very thin layer of initially subducted sediments (e.g., Tonga), could be caused by effective dehydration/melting of the sediment package at depths too shallow to be supplied to the arc itself, physical accretion of sediment in the forearc, or because current techniques to detect the sediment component in arc lavas are either not sufficiently sensitive or yield ambiguous results.

Several recent studies have shown that thallium (Tl) isotope compositions of lavas in the Mariana, Aleutian and Ryukyu arcs provide a powerful and unusually sensitive tracer of sediment involvement during arc lava genesis (Nielsen et al., 2016; Prytulak et al., 2013; Shu et al., submitted). Thallium is a highly incompatible trace metal, whose chemical behavior is classically considered to mirror large ion lithophile elements such as Rb, Cs, and K, due to similarities in ionic radii (Shaw, 1952). Thallium abundances were first specifically investigated in arc environments by Noll et al. (1996). They sought to determine the fluid mobility of chalcophile and siderophile elements relative to boron in putative hydrothermal fluids associated with arc magmatism by analyzing a suite of lavas from seven subduction zones. However, they could not determine unambiguous co-variation of thallium with other notionally fluid mobile elements. Whilst there are clear indications of thallium's high fluid mobility in ore-forming fluids (Heinrichs et al., 1980), the extent of fluid mobility under subduction zone conditions remains unconstrained. Complicating matters is the possibility of thallium retention in accessory phases such as phengite in the residual slab (Nielsen et al., 2016; Prytulak et al., 2013). Whether or not thallium behaves as a lithophile or chalcophile element is also setting specific, with clear lithophile behavior demonstrated during magmatic processes, irrespective of tectonic setting (Prytulak et al., 2016; Prytulak et al., 2013) and chalcophile affinities found in mantle conditions and during incipient partial melting (Nielsen et al., 2014). Recent advances in the calibration and determination of thallium abundances by laser ablation (Jenner and O'Neill, 2012; Nielsen and

Lee, 2013; Nielsen et al., 2014) are a promising means to better-constrain elemental Tl behavior. In general, the power of thallium as a tracer lies in its vanishingly small concentrations in the mantle (<1ppb; see review in (Nielsen et al., 2017)) versus potential inputs to a mantle source.

Thallium has two stable isotopes that display a wide of range of fractionation in terrestrial environments (see review in (Nielsen et al., 2017)). Specifically, thallium isotopes can be used to quantify sediment fluxes from subducted slabs because pelagic sediments are highly enriched in Tl and display isotopic compositions that are heavier than the isotopically homogeneous upper mantle (Nielsen et al., 2016; Prytulak et al., 2013; Rehkämper et al., 2004). The heavy Tl isotope compositions of pelagic sediments are due to the large isotope fractionation that occurs when Tl sorbs to Mn oxides that form a ubiquitous component in deep-sea sediments (Nielsen et al., 2013; Rehkämper et al., 2004; Rehkämper et al., 2002). Most sections of oceanic crust altered by hydrothermal fluids at low temperatures (<100°C), on the other hand, display light Tl isotope compositions coupled with strong Tl enrichment (Coggon et al., 2014; Nielsen et al., 2006b; Shu et al., submitted). Given the disparate Tl isotopic reservoirs represented by pelagic sediments and AOC, Tl isotopes should enable distinction between AOC and sediment components in arc lavas. However, the Tl concentrations in pelagic sediments are, generally, one to two orders of magnitude higher than AOC (1000-5000 ng/g and 10-100 ng/g, respectively) and, therefore, even minor amounts of sediment might dominate the Tl budget of arc lava source regions. To date, arc lavas investigated for Tl isotopes show almost exclusively signatures consistent with addition of sediment to the arc mantle source region, which is expected to overwhelm the presence of any thallium signature of AOC (Nielsen et al., 2016; Prytulak et al., 2013; Shu et al., submitted). However, the arcs investigated for Tl isotopes had previously been shown based on other geochemical data to contain significant sediment components (Elliott et al., 1997; Kay and Kay, 1988; Shinjo et al., 2000). Hence these studies provided confirmation that sediment cycling in arcs can be traced with Tl isotopes. In addition, they also showed that the subduction process itself does not appear to fractionate Tl isotopes because the major inputs outboard of the arcs have very similar values to those found in the arc lavas. Thus, any stable isotope fractionation between residual slab, melts and fluids must be smaller than the Tl isotope variations of the subducting sediments that dominated these arcs. Such a conclusion is also consistent with other studies of high-T magmatic systems in Hekla, Iceland (Prytulak et al., 2016) and the Colahuasi deposit in Chile (Baker et al., 2010) where no systematic Tl isotope variations were observed that could be related to fractional crystallization or high-T fluid transport. Thallium isotopes are, therefore, likely to be an excellent source tracer in subduction zones.

Here we present new Tl isotope data for samples from the Tonga-Kermadec and Central American arcs. Although sediment subduction appears almost continuous along-strike in both arcs (Plank and Langmuir, 1998), sections have been hypothesized to have very minor or even absent sediment components (Carr et al., 1990; Hawkesworth et al., 1997; Morris et al., 1990; Patino et al., 2000; Regelous et al., 1997; Regelous et al., 2010). In addition, the nature of the subducted sediment is very different in the Tonga-Kermadec and Central American arcs. A relatively thin layer of pelagic clays accounts for the majority of the package subducted underneath the Tonga-Kermadec arc, whereas thick and discrete pelagic and carbonate sedimentary packages dominate outboard of the Central American arc (Patino et al., 2000; Plank and Langmuir, 1988). Therefore, these two arcs present a unique opportunity to investigate the ubiquity of sediment addition in subduction zones and if Tl isotopes are able to trace sediment additions where other geochemical parameters might only return ambiguous results.

2. Samples and background

2.1 Tonga-Kermadec

The Tonga-Kermadec arc is located in the Southwest Pacific Ocean stretching over 3000km from the Northern end of New Zealand to northwards to the Vitiaz Trench approximately 200km south of Samoa (Fig. 1). The subducting Pacific plate drilled at Deep Sea Drilling Project (DSDP) sites 595/596 consists of only 70 meters of mainly pelagic red and brown clays, rich in ferromanganese oxide minerals overlying Cretaceous age oceanic crust (Menard et al., 1983; Speeden, 1973). The thickness, and the proportion of continental clastic sediment increase southward along the trench towards New Zealand (Gamble et al., 1996). The Louisville Seamount chain subducts obliquely, intersecting the trench at the point where the Tonga and Kermadec arcs meet (Fig. 1). Volcaniclastic material from Louisville Seamount Chain (LSMC) is evidenced in the sediments found at DSDP Site 204 (Fig. 1), some of which bear geochemical resemblance to Louisville Seamount rocks (Ewart et al., 1998).

Previous studies of lavas in the Tonga-Kermadec arc have found clear signatures of sediment (for example, high $^{207}Pb/^{204}Pb$ for a given $^{206}Pb/^{204}Pb$) dominating most of the Kermadec arc (Ewart et al., 1998; George et al., 2005; Haase et al., 2002; Hawkesworth et al., 1997; Regelous et al., 1997; Turner and Hawkesworth, 1997), whereas the Tonga arc appears more influenced by an AOC component (Regelous et al., 1997; Regelous et al., 2010; Wendt et al., 1997) although sediment may also constitute a minor component (George et al., 2005). The two northernmost islands in the Tonga arc, Tafahi and Niuatoputapu, display strong Pb isotopic evidence suggesting that the LSMC is the primary source of Pb in these two islands (Regelous et al., 1997; Regelous et al., 2010; Turner and Hawkesworth, 1997). As a whole, the Tonga-Kermadec arc, therefore, displays along-strike chemical and isotopic variation that can be related to changes in the composition of the down-going plate and, in particular, large variations in the ratio between sediments and AOC supplied to the mantle wedge (Haase et al., 2002). With these previous findings in mind, it would be expected that Tl isotopes display substantial and systematic variation as a function of the composition of the subducted material along-strike in the Tonga-Kermadec arc.

We have measured Tl isotope compositions for a set of 30 subaerial lavas from 12 islands covering the entire length of the Tonga-Kermadec arc (Table 1). The majority of the samples are basalts or basaltic andesites complemented by five dacites and three andesites where less evolved samples were not available. All samples are likely less than a few 100ka in age. Most samples have previously been investigated for major and trace elements and some radiogenic isotopes (Ewart et al., 1998; Regelous et al., 1997; Regelous et al., 2010; Smith et al., 1988). Here, we also present new major elements and Sr and Nd isotope data for samples that did not already have published values (Table 1 and 2). We have also analyzed Tl isotopes for 12 representative sediment samples (Table 3) from DSDP Sites 204 and 596 located outboard of the Tonga portion of the arc (Fig. 1). These sediments have previously been the subject of detailed geochemical analyses (Ewart et al., 1998). The AOC subducted beneath the Tonga-Kermadec arc is presently not well sampled by any drill holes and we have not analyzed any samples that represent Tonga-Kermadec AOC. A previous study analyzed composite samples of AOC from ODP Hole 801C outboard of the Mariana arc that are similar in age to the oceanic crust subducted in the Tonga-Kermadec arc (Prytulak et al., 2013). However, the Tl isotope and concentration data for ODP 801C revealed very different values to those that have been found in ODP 504B, IODP U1301 and DSDP 442B (Coggon et al., 2014; Nielsen et al., 2006b; Shu et al., submitted). This discrepancy is possibly related to the unusual Top Alkali Basalt found in ODP Hole 801C, which would could have severely changed the Tl concentration and isotopic profile of the oceanic crust due to late hydrothermal systems associated with this magmatic activity. Hence, we assume that AOC in the Tonga-Kermadec arc is most likely similar to the majority of AOC sections investigated to date.

2.2 Central America

The Central American volcanic arc (CAVA), *sensu stricto*, results from the subduction of the Cocos and Nazca plate beneath the Caribbean Plate and extends some 1200km from western Guatemala to central Costa Rica (Fig. 2). The volcanic front terminates to the southeast where the Cocos Ridge subducts beneath central Costa Rica. From Guatemala to northwestern Costa Rica the Cococs plate consists of ~ 24 Ma oceanic crust formed at the East Pacific Rise. In contrast, further southeast along the CAVA slightly younger oceanic crust (15-20 Ma) of the Cocos-Nazca Ridge that is variably overprinted by Galapagos hotspot magmatism is subducting (Werner et al., 2003). Some of the physical parameters of the subduction system vary systematically along the strike of the arc. Most notably, variations in crustal thickness of the overriding plate, and of slab dip, have been used to help explain the unique along-strike variation in geochemistry along the CAVA (Abers et al., 2003; Carr, 1984; Carr et al., 1990; Feigenson and Carr, 1993; Patino et al., 2000).

The active arc front has produced magmas since the Quaternary (Carr et al., 2007) and can be structurally split into seven segments of aligned volcanic centers (Bolge et al., 2009; Stoiber and Carr, 1973), spaced an average of 28km apart, allowing for higher resolution sampling of volcanic products than most other convergent margins (Carr et al., 2003). Additional volcanic centers lie behind the active arc front, enabling the investigation of both along-strike, and cross-arc chemical variations (Geilert et al., 2012; Patino et al., 1997; Walker et al., 1995; Walker et al., 2000). Furthermore, the study of magmatic sources in the CAVA is aided by the unusual abundance of mafic lavas (Carr, 1984).

There are strong chemical constraints on the inputs to the system through a combination of ocean dredging and drilling. For instance, the downgoing Cocos plate has been the focus of numerous DSDP, Ocean Drilling (ODP) and International Ocean Drilling (IODP) expeditions (Fig. 2). The sedimentary package covering the Cocos plate is thought to be fairly homogeneous along the strike of the arc (Patino et al., 2000). The main lithologies are described from DSDP Leg 67 Site 495, drilled 22km seaward of the middle America trench, outboard of the Guatemala/El Salvador border (Aubouin et al., 1982; Plank and Langmuir, 1998). Site 495 consists of ~175m of hemipelagic sediments overlying ~250m of pelagic carbonate ooze (Aubouin et al., 1982). Both of these sediment lithologies have been invoked in the source of CAVA lavas (Patino et al., 2000). DSDP Hole 504B is also located in geographical proximity to the arc on the Nazca plate south of the Cocos ridge. Site 504 has one of the best-studied sections of in situ altered oceanic crust, and has been investigated by several drilling expeditions (Alt et al., 1996). Furthermore, altered basalts from Hole 504B provided the first evidence for light thallium isotopes in low temperature altered crust (Nielsen et al., 2006b).

The earliest investigations of mafic CAVA lavas revealed distinct and systematic along-strike variations in chemistry (Carr, 1984), which has encouraged intense subsequent investigation. In general, a symmetrical pattern with a maximum or minimum at Nicaragua is apparent in a number of chemical signatures such as Ba/La, B/La and Be isotopes, which is generally attributed to variations in sediment flux along the arc, with a maximum in Nicaragua and a minimum in Costa Rica and western Panama (where the Cocos ridge is being subducted)

(Carr, 1984; Carr et al., 1990; Leeman et al., 1994; Patino et al., 2000). Although reaching an apparent maximum in Nicaragua, the recycled sediment flux also shows its greatest variation in Nicaragua, which may explain the eruption of contrasting basaltic magmas in this portion of the CAVA (Walker et al., 1990; Walker et al., 2001).

More recent studies have confirmed and converged on the idea of an anomalous Nicaraguan segment, including arguments for the involvement of serpentinite-derived fluids in the heavily slab-influenced western Nicaraguan lavas (Eiler et al., 2005; Heydolph et al., 2012; Rupke et al., 2002; Sadofsky et al., 2008). The Costa Rican segment is also atypical with variable subducted inputs from the Galapagos plume (Gazel et al., 2009; Gazel et al., 2011; Hoernle et al., 2008; Sadofsky et al., 2008). Finally, higher resolution seismic data has allowed the more detailed examination of the tectonic relationship to volcanic location and chemical characteristics in the southern half of the arc (Abers et al., 2003; Hoernle et al., 2008; Syracuse et al., 2008; Van Avendonk et al., 2011). Thus the well-documented, strong and systematic chemical variations, in particular the rich background of fluid mobile element analysis such as B, Be and Li in the CAVA, make it an ideal place to test the ability of thallium isotopes to reflect individual slab components in the source of the lavas.

We have measured 34 lavas from the CAVA system and two sediments from DSDP Site 495. All but three lava samples (from Guatemala) are from the active volcanic front. Most are basaltic, with SiO_2 below 52 wt% and have been extensively studied by numerous investigations for major element, trace element and both radiogenic and stable isotope variations. An extremely useful chemical database has been compiled for CAVA lavas (Carr et al., 2014) and the chemical compositions and references for the samples of this study are archived in that database.

3. Methods

3.1 Sample preparation

All sediment samples and lavas from Central America as well as the majority of lavas from Tonga were received and processed as powders. Some of the lavas from Tonga-Kermadec were received as rock fragments and these were carefully crushed into mm-sized chips and handpicked under binocular microscope to avoid pieces with surficial alteration and contamination. Subsequently the separated chips were ultrasonicated in ultra-pure water and any particles in suspension were discarded. Separate aliquots of several of the rock chip samples were also subjected to mild leaching in 1M HCl in order to investigate if contamination from any Mn oxides or alteration minerals was present (Table 1). This procedure has been shown to effectively remove these contaminants (Nielsen et al., 2016).

The rock and sediment powders as well as the handpicked and cleaned chips were dissolved in a 1:1 mixture of concentrated distilled HNO_3 and HF on a hotplate at ~150°C for 24h. They were then dried and fluxed several times using a 1:1 mixture of concentrated distilled HNO_3 and HCl until the fluorides, which formed in the first step, were completely dissolved. Following this, samples were dried on a hotplate and dissolved in 1M HCl in preparation for separation of Tl from sample matrix. Isolation of Tl followed previously described anion exchange chromatographic methods (Nielsen and Rehkämper, 2011; Nielsen et al., 2004). Total procedural Tl blanks during this study were <3pg, which is insignificant compared to the indigenous Tl processed for the samples of >3ng.

3.2 Thallium isotope and concentration measurements

Thallium isotope compositions were determined using a Thermo Finnigan Neptune multiple collector inductively coupled plasma mass spectrometer (MC-ICPMS), located in the Plasma Facility at Woods Hole Oceanographic Institution (WHOI). Following previous studies (Nielsen et al., 2004), external correction for mass discrimination to NIST SRM 981 Pb and standard-sample bracketing to the NIST SRM 997 Tl standard were applied for measurement of Tl isotopic compositions and correction for instrumental mass bias. Thallium isotope compositions are reported relative to the NIST SRM 997 standard in parts per 10,000:

$$\varepsilon^{205}Tl = 10{,}000 \times (^{205}Tl/^{203}Tl_{sample} - {}^{205}Tl/^{203}Tl_{SRM\ 997})/(^{205}Tl/^{203}Tl_{SRM\ 997}) \quad (1)$$

The column chemistry procedure returns quantitative Tl yields (Nielsen et al., 2004; Prytulak et al., 2013; Rehkämper and Halliday, 1999), thus Tl concentrations were estimated by monitoring the ^{205}Tl intensity during the isotopic measurements. The measured $^{205}Tl/^{208}Pb$ ratios were converted directly into Tl concentrations by adding a known quantity of NIST SRM 981 Pb. Recent studies in the NIRVANA (Non-traditional Isotope Research on Various Advanced Novel Applications) lab at WHOI has documented that the long-term reproducibility of Tl isotopes and concentrations in silicate samples are ±0.4 $\varepsilon^{205}Tl$-units (2sd) and ±15% (2sd), respectively (Nielsen et al., 2015; Nielsen et al., 2016; Shu et al., submitted).

3.3 Measurements of Nd and Sr isotope compositions and major elements

For Sr and Nd isotope measurements, approximately 100 mg of sample was digested in concentrated HNO_3-HF, evaporated and treated with 15M HNO_3 until completely in solution. The sample was then dissolved in 3M HNO_3, and Sr and the REE were separated from the rock matrix using Eichrom SrSpec and TRUSpec resins, respectively. The REE fraction was redissolved in 0.25M HCl, and Nd separated from the other REE using ion exchange columns containing 1.5 ml of Eichrom LNSpec resin. All reagents used were Teflon distilled, and total procedural blanks were below 100 ng and 20 ng for Sr and Nd respectively. Isotope measurements were carried out on a Thermo Triton thermal ionisation mass spectrometer in static mode at the GeoZentrum Nordbayern. Measured $^{87}Sr/^{86}Sr$ and $^{143}Nd/^{144}Nd$ ratios were corrected for instrumental mass fractionation assuming $^{86}Sr/^{88}Sr$ = 0.1194 and $^{146}Nd/^{144}Nd$ = 0.7219. Over the period of analysis, average values of the NBS987 Sr and La Jolla Nd standards were $^{87}Sr/^{86}Sr$ = 0.710249 and $^{143}Nd/^{144}Nd$ = 0.511850, respectively, and the data in Table 1 were normalized to values of 0.710240 and 0.511857, for direct comparison with the earlier data from Ewart et al. (1998).

Major element analyses of Tonga lavas were carried out by XRF (AMETEK Spectro XEPOS Plus) at the GeoZentrum Nordbayern, on fused glass discs prepared by using lithium tetraborate as flux. Loss on ignition was determined on a 1 g aliquot heated at 1030°C in a muffle furnace for 12 hours.

4. Results

4.1 Tonga-Kermadec

Thallium concentration in the Tonga-Kermadec lavas range from ~5ng/g to 144ng/g, with the highest concentrations found for the most evolved samples (Fig. 3a). Lavas in the Tonga arc vary between $\varepsilon^{205}Tl$ = -0.7 to +6.7, with an average value of $\varepsilon^{205}Tl$ = +1.2, while lavas in the Kermadec arc vary between $\varepsilon^{205}Tl$ = -0.5 to +11.5 (Table 1), with an average value of $\varepsilon^{205}Tl$ = +3.1. Every lava analyzed in this study is significantly heavier than the average upper mantle, as defined by MORB, which displays $\varepsilon^{205}Tl = -2 \pm 0.5$ (Nielsen et al., 2006a; Nielsen et al., 2006b).

Sediments from DSDP Sites 204 and 596 contain primarily pelagic clays (Menard et al., 1983; Speeden, 1973), but at DSDP Site 204 significant amounts of volcaniclastic sediments from the LSMC are also found (Speeden, 1973). Thallium isotope compositions and concentrations are substantially different for these two sediment types with pelagic clays exhibiting a concentration-weighted average $\varepsilon^{205}Tl = +3.6$ and [Tl] = 1876 ng/g, whereas volcaniclastic sediments are characterized by concentration-weighted average $\varepsilon^{205}Tl = +0.2$ and [Tl] = 214 ng/g (Table 3). We use these averages as representatives for the two different sediment components and do not attempt to estimate the bulk average subducted sediment because the volcaniclastic sediment component is highly variable along the arc to the extent that little or no LSMC volcaniclastics are subducted beneath the Kermadec arc. The Tl compositional differences are consistent with substantial enrichment of isotopically heavy Tl in pelagic clays from Mn oxides (Nielsen et al., 2013; Rehkämper et al., 2004), whereas volcaniclastic sediments only contain minor Mn oxide components.

4.2 Central America

Thallium concentrations in the CAVA lavas range from <5 ng/g in primitive lavas from central Nicaragua to ~150 ng/g in more evolved lavas (Table 4). This behavior likely reflects the near-perfectly incompatible behavior of Tl during differentiation processes (Prytulak et al., 2016). Although the lavas span a large geographic area and encompass many volcanic centers, the overall sense of increasing Tl concentration with decreasing MgO is apparent (Fig. 3b). A clear exception is sample CR-IZ-D6 from Irazu volcano in Costa Rica, which has an anomalously high thallium concentration (243 ng/g) for its degree of evolution (Fig. 3b). Note that we did not estimate the Tl concentration of sample NE203. This sample was analyzed by

Noll et al. (1996) who reported a concentration of 1 ng/g. However, this concentration is substantially lower than any other arc lava analyzed to date and also produces Ce/Tl = 8400, which is far higher than what is realistic for an arc lava. We, therefore, only use the Tl isotope composition for this sample.

Compared to other investigated arcs, thallium isotope signatures lighter than MORB are more common in the CAVA (Table 4). At face value, the 34 lavas analyzed in this study also display the largest range of isotope composition in mafic lavas documented to date, with ε^{205}Tl = -11.5 to +9.0 and does not correlate with classic recycled sediment indicators such as Ba/La, U/La or ^{10}Be in the arc. The extremes of this range occur in the same volcanic system, the Nejapa cinder cones of central Nicaragua, which are noteworthy for their overall chemical variability (Walker et al., 1990; Walker et al., 2001). Significantly light isotope signatures of ε^{205}Tl = -8.2 are also found in Irazu volcano, located in central Costa Rica. The three behind the volcanic front sample from Guatemala (GU-C201, GU-C303 and GU-C837) have average ε^{205}Tl = -1.1, which is not significantly anomalous when considered in the context of the overall variation in CAVA lavas. The carbonate sediment yields a heavy isotope value of ε^{205}Tl = +5.8, albeit at a low Tl concentration of 33 ng/g. The hemipelagic sediment has a much higher thallium concentration of 1077 ng/g and an isotope composition of ε^{205}Tl =+0.2, similar to sediments analyzed from outboard the Mariana, Aleutian, and Tongan subduction zones.

5. Discussion

5.1 Effects of secondary processes on primary [Tl] and ε^{205}Tl

It has been documented that processes such as degassing, subaerial aqueous alteration, assimilation of wall rock and fractional crystallization prior to eruption can alter the Tl budget of subaerial lavas and potentially cause Tl isotope fractionation (Nielsen et al., 2016; Prytulak et al., 2013). Before interpreting isotopic signatures in terms of source components we must first assess if any of the above processes affected the investigated lavas from Tonga-Kermadec and Central America.

5.1.1. Subaerial aqueous alteration

Subaerial lavas are often observed to preferentially lose alkali metals during aqueous alteration from meteoric water (Schiano et al., 1993). This effect is most likely due to the high solubility of these metals in aqueous solution. Given the geochemical similarity between Tl and the alkali metals (i.e. ionic charge and radius as well as high aqueous solubility) it has been suggested that subaerial alteration may lead to significant Tl losses, reflected as high Ce/Tl ratios coupled with high Th/Rb ratios (Nielsen et al., 2016). These losses, however, would likely not be associated with Tl isotope fractionation because weathering has been shown to cause negligible effect on the isotope system (Nielsen et al., 2005). Figure 4 illustrates the trajectory of alteration in Ce/Tl vs Th/Rb space with a Hawaiian lava that had clear petrologic and geochemical evidence for subaerial alteration although no Tl isotope fractionation appeared to have perturbed this sample (Nielsen et al., 2006a). Also plotted is one sample from the Aleutians that likewise was suspected of subaerial alteration (Nielsen et al., 2016). Compared to these two lavas, the datasets from both Tonga-Kermadec and the CAVA do not show any clear indication of subaerial alteration. High loss on ignition (LOI) measured for bulk rock powders can also be a qualitative indicator of degree of weathering, but in our data set there are no correlations between LOI and other indicators of weathering and generally LOI is very low (<0.5%) for the studied lavas, which suggests that alteration is not significant.

Central American lavas span greater ranges of Ce/Tl and Th/Rb than unaltered lavas from the Tonga-Kermadec and Aleutian arcs (Fig. 4). In principle, this variation could be interpreted to reflect more extensive alteration of CAVA lavas. However, the vast majority of the samples studied here are historical eruptions with essentially no or very minor alteration (Carr et al., 2014), which suggests that the most elevated Th/Rb and Ce/Tl ratios of samples from Irazu volcano in central Costa Rica are likely related to their unusual Galapagos-tainted source rather than an alteration affect (Gazel et al., 2009; Gazel et al., 2011). This interpretation is also supported by the high Th/Rb ratios observed in Galapagos lavas (Saal et al., 2007). Although no Tl concentration data is available for Galapagos lavas, high Ce/Tl ratios are generally found in other OIBs (Nielsen et al., 2014), which supports such an origin for the anomalous Ce/Tl and Th/Rb ratios found in the Irazu samples. Hence, we conclude that none of the CAVA samples were significantly affected by post-eruption aqueous alteration

5.1.2 Degassing

Volcanic fumaroles contain elevated concentrations of thallium and display a range of Tl isotope compositions that span both very light and heavy values, which has been interpreted to reflect both evaporation and condensation processes (Baker et al., 2009). In principle, degassing should be expressed as a loss of Tl associated with kinetic isotope fractionation whereby the light Tl isotope would preferentially be lost. Given that Tl partitioning during mantle melting is similar to Ce (Nielsen et al., 2014), it could be inferred that unusually high Ce/Tl ratios, not otherwise explained by aqueous weathering, coupled with heavy Tl isotope compositions are indicative of significant degassing - if lavas of the same degree of evolution and fractionating assemblage are compared. Such effects have been reported for arc lavas (Nielsen et al., 2016), but the lack of systematic Tl isotope fractionation for volcanic fumaroles also suggests that degassing might not be ubiquitously associated with significant Tl isotope fractionation (Baker et al., 2009). Within the present data set only one sample (Macaulay 10380) exhibits anomalously high Ce/Tl relative to the other samples (at similar MgO) in this study (Fig. 4b). The sample is also characterized by a heavy Tl isotope composition, as would be expected for a degassed lava. However, a second sample from Macaulay (Table 1) has an almost identical Tl isotope composition with a substantially lower Ce/Tl ratio, which would suggest that Tl loss due to degassing in this sample might not have been accompanied by significant Tl isotope fractionation and thereby consistent with published Tl isotope data for volcanic fumaroles (Baker et al., 2009). In addition, the Ce/Tl ratio of Macaulay 10380 is lower than the upper mantle (Fig. 4b), which implies that any Tl loss due to degassing was relatively minor.

Higher Ce/Tl ratios are found in the CAVA than in Tonga-Kermadec, (Fig. 4b), the Aleutians and Marianas (Prytulak et al., 2013). None of the high Ce/Tl ratios are associated with systematically heavy Tl isotope compositions, as would be expected for kinetic isotope fractionation associated with degassing. However, some of the highest Ce/Tl lavas in central Nicaragua also have the most extreme positive (ε^{205}Tl = +9.0) and negative (ε^{205}Tl = -11.5) thallium isotope compositions (samples NE-201 and NE-202; Fig. 4b), which mimics some of the most fractionated Tl isotope effects observed for volcanic fumaroles (Baker et al., 2009). The Tl isotope variations in volcanic fumaroles were even found to be large within individual volcanic centers (e.g. Kilauea volcano, Hawaii) (Baker et al., 2009), which suggests that lavas with very low Tl concentrations could more easily be perturbed to both heavier and lighter Tl isotope compositions by effects from degassing/condensation. Given that these two samples originate from neighboring Nejapa cinder cones and both have been classified as high-Ti basalts by Walker et al. (1990) with almost identical Sr and Nd isotopes (Carr et al., 2014), it seems improbable that the Tl isotope composition of these two samples reflect that of their mantle source. The lava sample GR5 also has similar major and trace element characteristics including anomalously low thallium concentration and heavy isotope composition (ε^{205}Tl = +3.5; GR5), which we also suspect could be influenced by kinetic processes rather than a true reflection of mantle source.

5.1.3 Assimilation and fractional crystallization

Thallium behaves as a near-perfect incompatible element during fractional crystallization of anhydrous phases with no resolvable Tl isotope fractionation (Nielsen et al., 2016; Prytulak et al., 2016). However, crystallization will affect key trace element ratios involving Tl as well as other elements (e.g. Ce/Tl, Ce/Pb, Sr/Nd, U/Nb) due to systematic differences in the mineral-melt partition coefficients (Blundy and Wood, 2003). In addition, any concomitant wall rock assimilation is likely to both affect these trace element ratios and potentially alter the Tl isotope composition of the original melt if the wall rock is isotopically different to the primitive melt.

Fractional crystallization affects all lavas, and our Tonga-Kermadec dataset contains andesites and dacites that will have undergone more extensive fractionation. Therefore trace element ratios should first be assessed for the effect of fractional crystallization. This is not a straightforward task because the samples are not genetically related along a shared liquid line of descent. However, the only trace element ratio that is systematically different in dacites relative to less evolved samples is Sr/Nd, which is lower in dacites, likely due to crystallization of plagioclase. No elemental ratios involving Tl are significantly different in dacites, suggesting that Tl and most other trace elements (except for Sr) behaved highly incompatibly. Therefore trace element ratios using thallium can be employed to investigate the sub-arc mantle and contributions from the subducting slab in the Tonga-Kermadec system. In addition, there are no differences between Tl isotope compositions measured for dacites and less evolved samples in the Tonga-Kermadec system (Table 1). The dacite sample from Curtis Island is the isotopically lightest sample from the Kermadec arc, which could be interpreted to reflect assimilation of isotopically light wall rock material, although it is difficult to envision a process that created a light Tl isotope signature in the first instance, since igneous ocean crust is isotopically similar MORB (Nielsen et al., 2006b) whereas lower arc crust in the Tonga-Kermadec arc is most likely heavier than MORB as evidenced by the overall heavy values observed in the lavas. However, such an interpretation is consistent with the fact that this sample exhibits the most radiogenic Sr isotope composition compared with other islands in the Tonga-Kermadec arc combined with Nd isotope compositions similar to other Kermadec islands (Ewart et al., 1998), which might indicate assimilation of older oceanic crust. However, given that the basaltic andesite (Table 1 and 2) displays Tl isotope and other basalts from Curtis Island display Pb, Sr and Nd isotope compositions that are identical to dacites and rhyolites from the same island (Ewart et al., 1998; Smith et al., 1988), we infer that assimilation processes are unlikely to have affected isotopic compositions of Tl, Sr, Nd or Pb for these samples.

The nature of our sample set from the CAVA is generally a single sample per volcanic edifice, which again makes evaluating the effects of fractional crystallization difficult.

Furthermore, the well-documented, high amplitude variation in the chemical characteristics of the source regions combined with a variable sediment flux along the arc, mean that variation in trace element ratios such as Ce/Tl, Ce/Pb, Sr/Nd, and U/Nb yield real information about source rather than a reflection of secondary fractionation. The typical petrographic assemblage documented in the CAVA are large, zoned plagioclase and pyroxene crystals in more evolved magmas with ubiquitous olivine and magnetite in basaltic lavas, and only very rare reports of amphibole in high Na lavas from Guatemala (Carr et al., 2003; Walker et al., 2000). Thus, the assemblage is very similar to those investigated for the effects of differentiation on Tl isotopes by Prytulak et al. (2016), where no correlation between thallium isotopes and indices of differentiation were found, and thallium remained near-perfectly incompatible throughout fractionation from basalt to rhyolite. Thus, we conclude that the dominant cause of trace element variation in the presented CAVA lavas is mantle source differences rather than magmatic processes. This conclusion is in agreement with previous studies that found silicic volcanic rocks in Central America show the same regional variations in trace element ratios that the basaltic rocks do (Vogel et al., 2004; Vogel et al., 2006).

5.2 Slab components in Central America and Tonga-Kermadec lavas

5.2.1. Pelagic sediment contributions throughout Tonga-Kermadec

As outlined above, secondary processes are unlikely to account for much, if any, of the Tl isotope variation observed in the Tonga-Kermadec lavas. Therefore, the mantle source region along the entire length of the arc is characterized by Tl isotope compositions heavier than the depleted upper mantle and AOC (Fig. 6). This provides clear evidence for a contribution of Tl from subducted sediment in all Tonga-Kermadec lavas. In general, pelagic sediments display substantial Tl isotope variation (e.g., Rehkamper et al., 2004; Nielsen et al., 2016). It is, therefore, difficult to assess the exact Tl isotope composition of the sedimentary endmember in the Tonga-Kermadec arc, which prevents a direct utilization of Tl isotopes to quantify sediment contributions. Visually, it appears that Kermadec lavas are isotopically heavier than Tonga lavas (Fig. 6), which might suggest a larger sediment component in the Kermadec lavas than in Tonga. This observation is also generally supported by evidence from radiogenic isotopes (Regelous et al., 1997) that suggest greater sediment contributions in Kermadec than in Tonga lavas (Fig. 7). However, increased sediment contribution in the Kermadec arc versus Tonga should result in higher Tl concentrations at a given MgO, which is not observed (Fig. 3a). The small difference in Tl isotopes between Kermadec and Tonga is, therefore, more likely related to differences in the average Tl isotope composition of subducted sediments.

Two of the lava samples investigated here extend to even heavier Tl isotope compositions than observed for pelagic sediments (Fig. 6). These more extreme values could potentially be explained by the occurrence of ferromanganese (Fe-Mn) nodules in the subducted sediment pile (Menard et al., 1983; Speeden, 1973) that in other locations have been observed to exhibit Tl concentrations as high as 100 μg/g and ε^{205}Tl > +10 (Nielsen et al., 2016; Rehkämper et al., 2004; Rehkämper et al., 2002). Although the Sr, Nd and Pb concentrations of these nodules are also high (Hein et al., 2000), their concentrations relative to Tl are sufficiently low that addition of small amounts (<0.01% by weight) of pure Fe-Mn nodule material to the arc lava source region would only have a minor effect on Sr, Nd and Pb isotopes whereas the contaminated mantle source region would strongly inherit the Tl isotope signature of the Fe-Mn nodule (Fig. 7). The extreme Tl isotope variation in the investigated lavas, therefore, suggest that transfer of material from slab to mantle wedge still contained sufficient heterogeneity to leave Tl isotope values highly variable. Most islands in the Tonga-Kermadec arc display only little variation in Sr and Nd isotopes (Ewart et al., 1998; Hergt and Woodhead, 2007; Regelous et al., 1997; Regelous et al., 2010; Turner et al., 2012), which suggests that the mantle source for each island is fairly homogenous. However, given the high Tl/Sr and Tl/Nd ratios for Fe-Mn nodules, heterogeneous addition of sufficient Fe-Mn nodule material to generate the observed Tl isotope variation would not register notably in Pb, Sr and Nd isotopes (Fig. 7).

Pelagic sediments clearly dominate the Tl budget of the subducted sediment package as evidenced by the heavy Tl isotope composition of lavas across the entire Tonga-Kermadec arc (Fig. 6), which is consistent with the recovered lithologies on the downgoing plate from DSDP Sites 595/596. Based on Tl isotopes it is also evident that pelagic sediments are present even in the Northern Tonga islands of Tafahi and Niuatoputapu where previous studies have found that LSMC material is an important source of Pb (Ewart et al., 1998; Regelous et al., 1997; Regelous et al., 2010; Turner and Hawkesworth, 1997). Although Pb isotopes in Tafahi and Niuatoputapu clearly point towards an influence of LSMC material, the Sr isotope composition of lavas from these two islands are significantly more radiogenic than LSMC material (Beier et al., 2011; Vanderkluysen et al., 2014), which requires an additional component with radiogenic Sr in the Northern Tonga mantle source. This component could be sourced from the Samoan mantle plume (Wendt et al., 1997), but given the heavy Tl isotope compositions also observed in Northern Tonga (Fig. 7), at least some of the more radiogenic Sr must originate from small amounts of pelagic sediment (<1% by weight). The small sediment component in northern Tonga is in agreement with several previous studies that found evidence for sediment involvement across the entire Tonga-Kermadec arc even in the Northern islands of Tafahi and Niuatoputapu (George et al., 2005; Hergt and Woodhead, 2007).

5.2.2. Central American isotope variations

Although the CAVA has large variations in thallium isotopes (Fig. 8a), without two anomalous regions (Central Nicaragua and Irazu volcano) and the three samples from behind the volcanic front, the average isotope composition is $\varepsilon^{205}Tl = -1.6 \pm 3$ (n=23), which, although variable, is identical within error to the upper mantle as represented by MORB ($\varepsilon^{205}Tl = -2 \pm 1$; Nielsen et al., 2006a). We have only measured two sediment samples from DSDP 495, but they represent the two major subducting lithologies (carbonate and hemipelagic sediment). The carbonate sample has a very low thallium concentration (33 ng/g) and a heavy isotope composition of +5.8. Investigation of corals, foraminifers, and biogenic oozes suggest that Tl concentrations of such materials is much lower than our carbonate sample (Nielsen and Rehkamper, 2011; Rehkamper et al., 2004). Furthermore, rivers draining carbonate lithologies have isotopically light thallium consistent with pure carbonate inhereting the seawater Tl isotope composition of $\varepsilon^{205}Tl = -6.0$ (Nielsen et al., 2005). Therefore, the heavy Tl isotope signature is probably inherited from manganiferous clay that is reported to occur within this carbonate unit (Aubouin et al., 1982). Whatever the cause of the heavy isotope composition of our single carbonate sample, the total budget of thallium subducting in the carbonates is likely not sufficient to perturb the overall Tl isotope budget.

5.2.3. Nicaraguan lavas: evidence for sediments?

Nicaragua has long been recognized as a location of chemically distinct lavas. For example, samples from Central Nicaragua are characterized by some of the highest $^{10}Be/^{9}Be$ ratios (Fig. 8b) found in arc lavas globally, which provides unequivocal evidence that hemipelagic clays found outboard of the CAVA contribute to magmatism in Nicaragua (Morris et al., 1990; Tera et al., 1986). Furthermore, many studies have concluded that Nicaraguan volcanoes have the strongest 'slab signature' in the CAVA, classically represented as elevated Ba/La ratios (Fig. 8c) that are found to peak in Western Nicaragua approximately between the volcanoes Cosiguina and Cerro Negro (e.g. Carr et al., 2003; Walker and Gazel, 2014). Ba/La ratios have commonly been employed as a proxy for a slab fluid component (Sadofsky et al., 2008; Walker et al., 2000; Woodhead et al., 1998; Woodhead and Johnson, 1993), which suggests that a high fluid flux could be responsible for the elevated Ba/La in Nicaraguan lavas. This inference is supported by several investigations that have invoked a higher fluid flux and significantly larger degree of melting beneath Nicaragua compared to the rest of the CAVA, due to the steep dip (~75^0) of the Cocos slab (Abers et al., 2003; Carr et al., 1990; Patino et al., 2000; Sadofsky et al., 2008; Syracuse et al., 2008). However, the regional variation in Ba/La actually reflects variation in La concentrations in the lavas, not Ba, and thus it is difficult to relate to a variable fluid flux, but could denote unusually high degrees of melting that vary as a function of fluid flux (Carr et al., 1990; Carr et al., 2007). Alternatively, given that the subducting sediments are characterized by extremely high Ba/La, it is also possible that the Nicaraguan peak in Ba/La is largely sediment related (Patino et al., 2000).

Figure 8b shows the along-strike variation of thallium isotopes without the three samples whose thallium isotope composition we suspect to be affected by kinetic processes (section 5.1.2). In Western Nicaraguan lavas, where Ba/La is at it highest, samples have average thallium isotopes of $\varepsilon^{205}Tl = -1.4 \pm 0.7$ (n=6), which is indistinguishable from the mantle value. Therefore, arguably the greatest slab input does not correspond to heavier Tl isotopic compositions as would be expected if this component was dominated by hemipelagic sediments with high Tl concentrations. The very elevated Ba/La (and Ba/Th) ratios in Western Nicaragua could, however, be sourced from carbonate sediments where Tl concentrations are low and, therefore, do not significantly affect the total Tl budget. This offers an explanation for the lack of co-variation between thallium isotopes and trace element indices of overall slab contributions in Nicaragua.

Central Nicaragua is the location of the Nejapa and the Granada volcanic fields, from which we have discounted three out of six samples. These fields are made up of cinder cones aligned along fault traces rather than large composite volcanoes. Erupted lavas are generally very primitive, high degree melts, with high MgO contents and very low concentrations of incompatible elements, including thallium (Table 4). A subset of the Nejapa and Granada lavas are characterized by an almost MORB-like absence of negative HFSE anomalies and have been dubbed high-Ti basalts (Walker et al., 1990). These higher-Ti compositions could be, in part, a product of re-melting mantle that had already generated LREE-enriched magmas, which might explain the extremely low concentrations of many incompatible elements (Carr et al., 1990; Feigenson and Carr, 1993; Reagan et al., 1994). Such a depleted mantle would also be more susceptible to contamination with components characterized by anomalous Tl isotope compositions.

The samples we include from this region are isotopically heavy with compositions of $\varepsilon^{205}Tl$ = -1.2, +0.1, +1.0 and +4.7. These values are indicative of recycling of hemipelagic sediment in the region, which is consistent with the generally elevated ^{10}Be values seen for this section of the CAVA (Fig. 8b). However, only one of these three samples has been analyzed for ^{10}Be and was found to be fairly low (Carr et al., 2014) and there is, therefore, no direct correlation between ^{10}Be and Tl isotopes (Fig. 8). It is important to note that correlations between these two parameters need not be apparent because ^{10}Be is high only in the youngest sediments, while Tl isotopes are likely heavy throughout the hemipelagic clays.

From the perspective of Tl isotopes, an attractive feature of Central Nicaragua is that with a locally trace element depleted mantle, the smallest addition of Tl from AOC, hemipelagic sediments, and/or serpentinite-derived fluid (which might be isotopically heavy in Tl; (Nielsen et al., 2015)) will dominate the Tl isotope signature, without being apparent in many other tracers. Thus, Central Nicaragua could be a tremendously fruitful area for further systematic examination, requiring more data on Cocos plate sediments and crust, oceanic serpentinites and Nicaraguan volcanic rocks.

5.2.4. Irazu, Costa Rica: evidence for altered oceanic crust?

Costa Rican lavas are notable in that not a single sample is isotopically heavy compared to the mantle as represented by MORB, and the general tendency towards isotopically light thallium (Fig. 8a) contrasts with all previously studied arcs. Irazu volcano in Costa Rica is further unique in a number of respects. The volcano lies at the southeastern terminus of the arc as well as in the path of subducting Galapagos-tinged crust. Two studies (Benjamin et al., 2007; Sadofsky et al., 2008) have examined olivine-hosted melt inclusions for major, trace, and volatile contents. Both note the high water contents of Irazu compared to many other volcanic centers in the CAVA. In particular, Irazu was the exception in the study of Sadofsky et al. (2008) because, unlike the rest of the investigated CAVA melt inclusions, Irazu did not show positive correlation of Ba/La and B/La and water contents. It also has the highest F contents for a given olivine composition coupled with the lowest B/La, Ba/La and highest La/Y, Nb/Y. Sadofsky et al. (2008) explained these unusual features as resulting from a very fluid rich, but sediment poor mantle, which is consistent with the subduction of sediment-poor seamounts at its present day location. They also raised the possibility of melting the altered mafic crust to explain the high La/Y and Nb/Y, which is consistent with regional isotopic and trace element studies (Gazel et al., 2009; Gazel et al., 2011; Hoernle et al., 2008). Our study shows that sample CR-IZ-D6 has the highest Tl concentration in the CAVA (243 ng/g), coupled with an extremely light isotope signature of $\varepsilon^{205}Tl = -8.2$. Thus the thallium concentration and isotope systematics are consistent with previous interpretation of incorporation of altered oceanic crust. Irazu specifically, and Costa Rica in general, may be one of the few regions where the downgoing oceanic crust is sufficiently naked of Tl-rich sediments to allow detection of isotopically light Tl derived from the AOC.

6. Inter-arc comparisons and implications for Tl subduction cycling

6.1. Sediment control of arc lava Tl budgets

As outlined in the introduction, there is overall consensus that both sediment and AOC components are actively transported from the subducting slab to the mantle wedge and participate in melt generation. However, even though sediment subduction is almost ubiquitous some arcs display highly attenuated sediment signatures (Plank and Langmuir, 1998).

Compilation of all arc lava Tl isotope data published to date reveals that the vast majority of samples plot towards heavier compositions than the DMM, which strongly implicates sediment in these arcs (Fig. 9). The only exceptions are the Western Aleutians and Costa Rica. Magmatism in the Western Aleutians likely reflects an unusual tectonic environment where orthogonal subduction of the Pacific plate has stalled significantly, which may have heated up the oceanic crust sufficiently to cause eclogite melting and eruption of adakitic magmas (Kay, 1978; Yogodzinski et al., 2015; Yogodzinski et al., 1995; Yogodzinski et al., 2001). As such, this section of the subduction zone represents a thermally anomalous environment where the uppermost portions of the subducted slab (sediments and some AOC) could have been removed by previous generations of magmatism, leaving the residue almost devoid of sediment (Kelemen et al., 2003). In addition to trace element (high Sr/Y) and radiogenic isotope data (Sr, Nd, Pb) that suggest slab melting is occurring there (Yogodzinski et al., 2015), the lack of heavy Tl isotope compositions in the Western Aleutians also imply that sediment is not actively involved in arc magma generation in this location (Nielsen et al., 2016). As discussed above, lavas from Costa Rica also display a significant population of light Tl isotope compositions (Fig. 8a). These could be related to the subduction of the Cocos Ridge and/or seamounts to its North, which results in a thinner sediment cover for this portion of the subducted plate. In addition, sediments subducted underneath Costa Rica are dominated by carbonates with very low Tl concentrations. Hence, a minor sediment component in Costa Rica arc lavas might not dominate the overall Tl budget.

The absence of light Tl isotope compositions in Central and Eastern Aleutians, Tonga-Kermadec, Marianas and Central America north of Costa Rica is most easily explained if the Tl budgets of arc lavas almost ubiquitously contain sediment, which is in agreement with the subducted inputs in these arcs (Plank and Langmuir, 1998). Given that the Tl concentration of most sediment types (excepting biogenic carbonate and opal) are more than an order of magnitude larger than AOC (Coggon et al., 2014; Nielsen et al., 2006b; Nielsen et al., 2016; Prytulak et al., 2013; Rehkämper et al., 2004) even small amounts of sediment would render this component the dominant Tl contributor. However, Tl isotopes do not correlate with more conventional indices of sediment or fluid contributions from the slab such as Th/La and Ba/Th (Fig. 10). This lack of correlation could suggest that Tl fluxes from sediments are decoupled from other sedimentary components, for example via the preferential mobilization of Mn oxides where Tl is highly concentrated. Of course, both Tl isotope compositions and trace element ratios of subducted sediments vary significantly (Nielsen et al., 2016; Plank and Langmuir, 1998; Prytulak et al., 2013) such that mixing between mantle and different sediment components might not be expected to generate globally significant correlations with Tl isotopes. Alternatively, it is also possible that trace element signatures in arc lavas, in particular those that are fractionated in subduction zones like Ba/Th, are decoupled from the process of mixing slab material with the mantle wedge as inferred in models that invoke mélange melting (Marschall and Schumacher, 2012; Nielsen and Marschall, 2017).

Based on the currently available data for Tl isotopes in arc lavas, we conclude that there is strong support for almost ubiquitous sediment involvement in arc magma genesis. Investigations of Tl isotopes in additional volcanic arcs will further illuminate the effectiveness of Tl isotopes to trace sediment recycling and whether this process is as widespread as current data suggests.

6.2. Behaviour of Tl in slab material: fluids and accessory phases

Although sediments, in most subduction zones, contain the bulk of Tl in subducted slabs, the partitioning of Tl between slab and mantle wedge need not only be controlled by sediments. Fluids and accessory phases that impart characteristic trace element fractionation observed in subduction zones can originate from all portions of the subducted slab (Carter et al., 2015; Hermann and Rubatto, 2009; Johnson and Plank, 1999; Kessel et al., 2005; Skora and Blundy, 2010). Here, we use new and previously published Tl concentration data for arc lavas to investigate the controlling factors in determining Tl incorporation into arc magmas. When plotting all arc lavas where fractional crystallization of phases such as clinopyroxene and plagioclase are relatively minor (<55% SiO_2) a hyperbolic relationship between Cs/Tl and Sr/Nd as well as Ba/Th ratios can be seen (Fig. 11). Thallium has previously been hypothesized as a somewhat fluid mobile element (Noll et al., 1996), but the large ionic radius and univalent charge of Tl likely also makes it compatible in minerals with large cation sites such as phengite and phlogopite (Prytulak et al., 2013) that may be important phases in subducted slab material (Schmidt and Poli, 1998). Natural data for previously subducted oceanic crust from Tian Shan (van der Straaten et al., 2008) support this inference as Tl concentrations in these samples correlate almost perfectly with K, Rb, Cs and Ba concentrations (Fig. 12) that are all controlled by the abundance of phengite (van der Straaten et al., 2008). Based on these data, it follows that Tl partitioning in subduction zones is likely strongly affected by the presence or absence of phengite in the slab residue. The stability of phengite is itself strongly dependent on the presence of fluids, with excess water lowering its stability or at least causing it to melt out at lower pressures and temperatures (Hermann and Green, 2001). Therefore, high fluid abundances tend to de-stabilize phengite at relatively lower temperatures and pressures. Thus, we interpret the hyperbolic relationship between Cs/Tl and Ba/Th (Fig. 11) in terms of the stability of phengite relative to the abundance of fluid present during melting. In this scenario, relatively lower Ba/Th and higher Cs/Tl would indicate that phengite is stable in the arc lava residue. No known subduction zone inputs display Cs/Tl as high as lavas in this portion of the diagram (Fig. 11), which requires that Cs and Tl be fractionated during subduction processing. In both natural rocks and experiments Cs has been shown to be the least compatible alkali metal in phengite (Busigny et al., 2003; Hermann and Rubatto, 2009; Melzer and Wunder, 2000) and, given that the ionic radius of Tl is most similar to that of Rb (Shannon, 1976), we predict that Tl is more compatible in phengite than Cs. This difference in phengite partitioning can explain the unusually high Cs/Tl ratios observed in many arc lavas (Figs. 5 and 11).

The absolute value of Ba/Th will be highly dependent on the initial Ba/Th ratio of sediments, which can vary by more than an order of magnitude due to the presence of barite in marine sediments (Plank and Langmuir, 1998). However, as the fluid abundance increases phengite will de-stabilize and partitioning of elements like Ba, Cs and Tl will become entirely dominated by the fluid, whereas Th will be controlled by partitioning into accessory phases like monazite that can accommodate it (Hermann and Rubatto, 2009). Similarly, uniformly higher Sr/Nd ratios relative to subduction zone inputs (Fig. 11b) is likely controlled by retention of Nd in monazite or another REE-rich phase (Hermann and Rubatto, 2009; Skora and Blundy, 2012). However, higher fluid fluxes could more effectively remove Sr from the slab (Kessel et al., 2005) and thus further enhance the Sr/Nd fractionation. At high fluid fluxes, phengite destabilizes and without a phase that can realistically retain Cs and Tl in the residue, the fluid will most likely contain most of the Cs and Tl in the system and, therefore, obtain the Cs/Tl ratio of the bulk slab material it was released from. This process would explain why Cs/Tl ratios are generally in the range of subduction zone inputs for arc lavas that are characterized by high Ba/Th and Sr/Nd. Although mechanistically somewhat different, this interpretation could be compatible with models of arc trace element fractionation where fluid fluxes are relatively uniform across arcs and variations in sediment abundance in the subducted slab controls ratios of fluid mobile elements such as Sr/Nd and Ba/Th (Elliott, 2003). In this interpretation, high Sr/Nd and Ba/Th would be observed for arc regions with low sediment abundances. However, low sediment abundances would likely also produce less phengite that would probably melt out earlier than in high sediment arc sections and thus produce low Cs/Tl. Hence, it is currently not directly possible to distinguish between variations in sediment abundance in the slab (Elliott, 2003) and presence of excess fluid relative to phengite as implied here by Figure 11. In fact, the two scenarios do not appear to be mutually exclusive.

Further support for the involvement of phengite in controlling the Tl concentration of arc lavas is found in the slight tendency of heavy Tl isotope compositions in arc lavas to be associated with higher Cs/Tl ratios (Fig. 5). Such a relationship is expected in arcs where sediments contain high potassium concentrations (e.g. Aleutians, Tonga-Kermadec, Marianas), which will favor phengite formation. Phengite is also stable in eclogitized oceanic crust (Carter et al., 2015; van der Straaten et al., 2008) and metamorphosed continentally derived detrital sediments (Hermann and Rubatto, 2009), which have ε^{205}Tl $\leq$ -2. Therefore, high Cs/Tl ratios need not exclusively be associated with heavy Tl isotopes in order to be explained by residual phengite.

7. Conclusions and outlook

We present Tl isotope data from the Tonga-Kermadec and Central American arcs. Lavas from Tonga-Kermadec are offset in one direction from the mantle towards the heavy Tl isotope compositions that are observed in pelagic clays in drill cores outboard of the arc. The Tl isotope data show that sediments dominate the Tl budget of the subarc mantle in this arc.

The Tl isotope budgets of Central American lavas are influenced both by subducted sediments and AOC. Specifically, we find evidence for involvement of hemipelagic sediments in Central Nicaragua whereas Costa Rican lavas bear a strong influence from AOC. The lack of a sediment signature in Costa Rica may be related to a thinner sediment where the Cocos ridge and associated seamounts are subducted as well as the predominance of carbonates in the sediment package that contain very low Tl concentrations.

Review of Tl isotope data from five arcs reveal that most lavas are displaced towards heavy values that indicate involvement of pelagic sediments. Detection of AOC with Tl isotopes is very limited, even for segments of arcs that have been hypothesized as dominated by AOC components. The almost absent AOC signature for Tl isotopes is likely due to the much higher Tl concentrations observed in pelagic sediments relative to AOC. Hence, Tl isotopic data for arc lavas that imply involvement of sediments should not be seen as evidence against involvement of AOC in their source regions. Rather, Tl isotopes appear to be an overall excellent tracer of subducted sediment as long as these contain sufficient Mn oxides to generate Tl isotope compositions heavier than the ambient mantle. Given that pelagic clays are very common within the subducted sediment package in most subduction zones (Plank and Langmuir, 1998), Tl isotopes promise to find utility in additional subduction zones. The almost ubiquitous sediment signature for Tl isotopes in arcs suggests that most arc segments actively cycle sediments to depth, which is consistent with observations of sediment subduction outboard of subduction zones worldwide (Plank and Langmuir, 1998). Further studies of a wider range of arcs in which sediment subduction might take place, will reveal if this conclusion holds true for subduction zones in general.

Lastly, we suggest that Tl partitioning relative to Cs in arcs is controlled by residual phengite during melting of slab components or, in cases where phengite is exhausted, fluids that carry the bulk of Tl and the alkali metals with them resulting in little net fractionation between Cs and Tl. This conclusion will benefit immensely from experimental verification involving different slab components such as sediments, AOC, serpentinite and mélange.

8. Acknowledgements

We would like to thank T. Horscroft and the editors of JVGR for the opportunity to write this paper. We gratefully acknowledge funding from NSF grants EAR-1119373 and EAR-1427310 to SGN.

FIGURE CAPTIONS

Figure 1. Map of the Tonga-Kermadec arc. Islands from which we have analyzed samples are marked with square symbols. Colours of symbols are the same as those used in Figures 3, 4, 5, 6 and 7.

Figure 2. Map of the Central American arc. All volcanoes from which we have analyzed samples are marked with coloured square symbol and the name of the volcano is indicated next to the symbol. Symbol colours are also used in Figures 3, 4, 5 and 8.

Figure 3. Thallium concentrations plotted against MgO in lavas from (a) Tonga-Kermadec and (b) Central America.

Figure 4. Ce/Tl plotted against Th/Rb ratios for lavas from Tonga-Kermadec and Central America. In (a) is also shown two lavas, one from Hawaii (Nielsen et al., 2006a) and one from the Aleutians (Nielsen et al., 2016), that were affected by subaerial alteration and loss of alkali metals and Tl. (b) is a close-up of the area that contains all the arc lavas from Central America. (c) close-up of the area that contains all the arc lavas from Tonga-Kermadec. Unaltered arc lavas from the Aleutians plot inside the pink field for comparison. DMM field is based on the average composition of global MORBs (Jenner and O'Neill, 2012). It is noteworthy that the Th/Rb ratios of Galapagos lavas (Th/Rb = 0.11 to 0.22 (Saal et al., 2007)) overlap with the values found in Irazu volcano.

Figure 5. Thallium isotope compositions plotted against Cs/Tl ratios for (a) Central America and (b) Tonga-Kermadec lavas. Also shown are fields for Aleutians and Mariana arcs.

Figure 6. Thallium isotope compositions of Tonga-Kermadec lavas along-strike in the arc. Also shown is the field for the depleted mantle (grey bar), pelagic clays (brown bar) and volcaniclastic sediments (pink bar). Volcaniclastic sediment subduction is only taking place in the Tonga portion of the arc and is, therefore, not extended to the Kermadec portion of the arc. The isotope compositions of the sediment components were calculated as concentration-weighted averages of the individual pelagic and volcaniclastic sediments analyzed (Table 3). Altered oceanic crust (AOC) is isotopically light and is indicated by an arrow.

Figure 7. Thallium isotope composition plotted against (a) $^{208}Pb/^{204}Pb$, (b) $^{87}Sr/^{86}Sr$ and (c) $^{143}Nd/^{144}Nd$ isotope compositions for the Tonga-Kermadec arc. Symbols for arc lavas are the same as in figure 1. Bulk mixing lines between the mantle and the pelagic and volcaniclastic sediment components are shown in bold and dashed black lines. Tick marks indicate the amount of sediment required to produce the relevant Tl, Pb, Sr and Nd isotope variations. The mantle wedge [Pb] = 0.034 μg/g, [Sr] = 9.8 μg/g, and [Nd] = 0.713 μg/g (Salters and Stracke, 2004) and $^{208}Pb/^{204}Pb = 37.7$, $^{87}Sr/^{86}Sr = 0.7025$, $^{143}Nd/^{144}Nd = 0.51315$ is estimated from the most depleted samples found in the Eastern Lau Spreading Center and the Valu Fa Ridge (Hergt and Woodhead, 2007; Pearce et al., 2007). The Pb, Sr, Nd and Tl isotope compositions of the sediment components were calculated as concentration-weighted averages of the individual pelagic and volcaniclastic sediments analyzed (Table 3). The concentrations of the two sediment components were calculated using the concentrations averages of the individual pelagic and

volcaniclastic sediments analyzed (Table 3) and the data in Ewart et al (1998). Also shown is bulk mixing line between mantle and Fe-Mn nodules (light brown) and the Louisville Seamount Chain (LSMC) in green. Concentration and isotope data for average LSMC rocks are averages of published data (Beier et al., 2011; Vanderkluysen et al., 2014) that yield values of [Pb] = 2.15 µg/g, [Sr] = 560 µg/g, and [Nd] = 36 µg/g and $^{208}Pb/^{204}Pb$ = 39.25, $^{87}Sr/^{86}Sr$ = 0.7039, $^{143}Nd/^{144}Nd$ = 0.5129. The Tl isotope composition for LSMC is estimated to be similar to AOC. Tick marks indicate the amount of bulk sediment or LMSC material required to produce the observed Pb, Sr, Tl and Nd isotope variations. Concentrations and isotope compositions for the Fe-Mn nodules were assumed to be [Pb] = 1000 µg/g, $^{208}Pb/^{204}Pb$ = 38.7, [Sr] = 1500 µg/g, $^{87}Sr/^{86}Sr$ = 0.709, [Nd] = 200µg/g, $^{143}Nd/^{144}Nd$ = 0.5124, [Tl] = 100 µg/g, $\varepsilon^{205}Tl$ = +12.

Figure 8. Along-strike variation of (a) Tl isotopes, (b) ^{10}Be and (c) Ba/La ratios for the CAVA. Tl isotopes and Ba/La ratios are for the same samples, whereas ^{10}Be data is a compilation of all available data from CAVA (Carr et al., 2014). Grey field is the isotope composition of the upper mantle as represented by MORB (Nielsen et al. 2006a). Most volcanic centers have only a single sample. Circles are drawn around those that have two or more samples. All lavas are from composite volcanoes of the active volcanic front except for 1) three Guatemala lavas from behind the front, designated 'BVF' and with a small black circle and 2) three samples from fault-aligned cinder cones of the Nejapa and Granada regions, between two of the CAVAs linear volcanic segments. Samples where both ^{10}Be and Tl isotopes have been measured are marked with a cross. There is no correlation between Tl isotopes and ^{10}Be even though there is a tendency for Tl isotopes and ^{10}Be to be most enriched in the Central Nicaragua

region of the arc. Two-sigma standard deviation uncertainty on Tl isotope measurements is ±0.4 epsilon units.

Figure 9. Probability distribution plotted for arc lavas from Aleutians, Marianas, Central America and Tonga-Kermadec. Shown is also the field for the mantle (grey bar) and the general direction that the isotope compositions of AOC and sediments plot in.

Figure 10. Thallium isotope compositions in arc lavas from Aleutians, Marianas, Central America and Tonga-Kermadec plotted against (a) Ba/Th and (b) Th/La. These trace element ratios have been suggested as indicators of fluid (Ba/Th) and sediment (Th/La) addition from the slab to the mantle wedge (Elliott, 2003; Elliott et al., 1997; Plank, 2005; Woodhead et al., 1998). Fields for average subducted sediment compositions are shown as boxes with same colors code as the arc lavas. Sediment data are from (Nielsen et al., 2016; Plank and Langmuir, 1998; Prytulak et al., 2013) and this study. Fields are also shown for DMM (Jenner and O'Neill, 2012; Nielsen et al., 2014) and AOC (Coggon et al., 2014; Kelley et al., 2003; Nielsen et al., 2006b).

Figure 11. Ratio of Cs/Tl plotted against (a) Ba/Th and (b) Sr/Nd for lavas from Aleutians, Marianas, Central America and Tonga-Kermadec. In (b) are also shown fields for the compositions of the mantle (Jenner and O'Neill, 2012), detrital and pelagic sediments (Plank and Langmuir, 1998) and AOC (Coggon et al., 2014; Kelley et al., 2003; Nielsen et al., 2006b). Fields for the sediment endmembers are not shown for Ba/Th because sediment Ba concentrations are extremely variable due to influence of barite deposition (Plank and Langmuir,

1998). Red arrows are also shown that indicate the general areas that arc lavas are expected to occupy at different degrees of phengite and fluid involvement.

Figure 12. Thallium concentration plotted against (a) barium, (b) cesium, (c) potassium in eclogites from Tian Shan (van der Straaten et al., 2008). The excellent covariations show that all these elements are controlled by the only K-bearing phase in the rocks, which is phengite.

References

Abers, G.A., Plank, T. and Hacker, B.R., 2003. The wet Nicaraguan slab. Geophys. Res. Lett., 30(2).

Alt, J.C., Laverne, C., Vanko, D., Tartarotti, P., Teagle, D.A.H., Bach, W., Zuleger, E., Erzinger, J., Honnorez, J., Pezard, P.A., Becker, K., Salisbury, M.H. and Wilkens, R.H., 1996. Hydrothermal alteration of a section of upper oceanic crust in the eastern equatorial pacific: a synthesis of results from site 504 (DSDP legs 69, 70, and 83, and ODP legs 111, 137, 140, and 148). Proc. ODP Sci. Results, 148: 417-434.

Aubouin, J., Von Huene, R. and al, e., 1982. Site 495: COCOS PLATE—MIDDLE AMERICA TRENCH OUTER SLOPE. DSDP Init. Repts., 67.

Baker, R.G.A., Rehkämper, M., Hinkley, T.K., Nielsen, S.G. and Toutain, J.P., 2009. Investigation of thallium fluxes from subaerial volcanism-Implications for the present and past mass balance of thallium in the oceans. Geochim. Cosmochim. Acta., 73(20): 6340-6359.

Baker, R.G.A., Rehkämper, M., Ihlenfeld, C., Oates, C.J. and Coggon, R.M., 2010. Thallium isotope variations in an ore-bearing continental igneous setting: Collahuasi Formation, Northern Chile. Geochim. Cosmochim. Acta., 74(15): 4405-4416.

Beier, C., Vanderkluysen, L., Regelous, M., Mahoney, J.J. and Garbe-Schonberg, D., 2011. Lithospheric control on geochemical composition along the Louisville Seamount Chain. Geochem. Geophys. Geosyst., 12.

Benjamin, E.R., Plank, T., Wade, J.A., Kelley, K.A., Hauri, E.H. and Alvarado, G.E., 2007. High water contents in basaltic magmas from Irazu Volcano, Costa Rica. J. Volcanol. Geotherm. Res., 168(1-4): 68-92.

Blundy, J. and Wood, B., 2003. Partitioning of trace elements between crystals and melts. Earth Planet. Sci. Lett., 210(3-4): 383-397.

Bolge, L.L., Carr, M.J., Milidakis, K.I., Lindsay, F.N. and Feigenson, M.D., 2009. Correlating geochemistry, tectonics, and volcanic volume along the Central American volcanic front. Geochem. Geophys. Geosyst., 10: doi: 10.1029/2009gc002704.

Busigny, V., Cartigny, P., Philippot, P., Ader, M. and Javoy, M., 2003. Massive recycling of nitrogen and other fluid-mobile elements (K, Rb, Cs, H) in a cold slab environment: evidence from HP to UHP oceanic metasediments of the Schistes Lustres nappe (western Alps, Europe). Earth Planet. Sci. Lett., 215(1-2): 27-42.

Carr, M.J., 1984. Symmetrical and Segmented Variation of Physical and Geochemical Characteristics of the Central American Volcanic Front. J. Volcanol. Geotherm. Res., 20(3-4): 231-252.

Carr, M.J., Feigenson, M.D. and Bennett, E.A., 1990. Incompatible Element and Isotopic Evidence for Tectonic Control of Source Mixing and Melt Extraction Along the Central-American Arc. Contrib. Mineral. Petrol., 105(4): 369-380.

Carr, M.J., Feigenson, M.D., Bolge, L.L., Walker, J.A. and Gazel, E., 2014. RU_CAGeochem, a database and sample repository for Central American volcanic rocks at Rutgers University. Geosci Data J, 1(1): 43-48.

Carr, M.J., Feigenson, M.D., Patino, L.C. and Walker, J.A., 2003. Volcanism and geochemistry in central America: progress and problems. In: J.M. Eiler (Editor), Inside the subduction

factory. Geophysical Monograph. American Geophysical Union, Washington DC, pp. 153-174.
Carr, M.J., Saginor, I., Alvarado, G.E., Bolge, L.L., Lindsay, F.N., Milidakis, K., Turrin, B.D., Feigenson, M.D. and Swisher, C.C., 2007. Element fluxes from the volcanic front of Nicaragua and Costa Rica. Geochem. Geophys. Geosyst., 8.
Carter, L.B., Skora, S., Blundy, J.D., De Hoog, J.C.M. and Elliott, T., 2015. An Experimental Study of Trace Element Fluxes from Subducted Oceanic Crust. J. Petrol., 56(8): 1585-1605.
Coggon, R.M., Rehkämper, M., Atteck, C., Teagle, D.A.H., Alt, J.C. and Cooper, M.J., 2014. Mineralogical and Microbial Controls on Thallium Uptake During Hydrothermal Alteration of the Upper Ocean Crust. Geochim. Cosmochim. Acta., 144: 25-42.
Eiler, J.M., Carr, M.J., Reagan, M. and Stolper, E., 2005. Oxygen isotope constraints on the sources of Central American arc lavas. Geochem. Geophys. Geosyst., 6: doi: 10.1029/2004gc000804.
Elliott, T., 2003. Geochemical tracers of the slab. In: J. Eiler (Editor), Geophysical Monograph. American Geophysical Union, pp. 23-45.
Elliott, T., Plank, T., Zindler, A., White, W. and Bourdon, B., 1997. Element transport from slab to volcanic front at the Mariana arc. J. Geophys. Res.-Solid Earth, 102: 14991-15019.
Ewart, A., Collerson, K.D., Regelous, M., Wendt, J.I. and Niu, Y.L., 1998. Geochemical evolution within the Tonga-Kermadec Lau arc back-arc systems: the role of varying mantle wedge composition in space and time. J. Petrol., 39(3): 331-368.
Feigenson, M.D. and Carr, M.J., 1993. The Source of Central-American Lavas - Inferences from Geochemical Inverse Modeling. Contrib. Mineral. Petrol., 113(2): 226-235.
Gamble, J., Woodhead, J., Wright, I. and Smith, I., 1996. Basalt and sediment geochemistry and magma petrogenesis in a transect from oceanic island arc to rifted continental margin arc: The Kermadec Hikurangi Margin, SW Pacific. J. Petrol., 37: 1523-1546.
Gazel, E., Carr, M.J., Hoernle, K., Feigenson, M.D., Szymanski, D., Hauff, F. and van den Bogaard, P., 2009. Galapagos-OIB signature in southern Central America: Mantle refertilization by arc-hot spot interaction. Geochem. Geophys. Geosyst., 10.
Gazel, E., Hoernle, K., Carr, M.J., Herzberg, C., Saginor, I., van den Bogaard, P., Hauff, F., Feigenson, M. and Swisher, C., 2011. Plume-subduction interaction in southern Central America: Mantle upwelling and slab melting. Lithos, 121(1-4): 117-134.
Geilert, S., Freundt, A., Worner, G. and Kutterolf, S., 2012. Geochemical differences between along-arc and across-arc volcanics in west-central Nicaragua. J S Am Earth Sci, 35: 38-50.
George, R., Turner, S., Morris, J., Plank, T., Hawkesworth, C. and Ryan, J., 2005. Pressure-temperature-time paths of sediment recycling beneath the Tonga-Kennadec arc. Earth Planet. Sci. Lett., 233(1-2): 195-211.
Haase, K.M., Worthington, T.J., Stoffers, P., Garbe-Schonberg, D. and Wright, I., 2002. Mantle dynamics, element recycling, and magma genesis beneath the Kermadec Arc-Havre Trough. Geochem. Geophys. Geosyst., 3: art. no.-1071.
Hawkesworth, C.J., Turner, S.P., McDermott, F., Peate, D.W. and vanCalsteren, P., 1997. U-Th isotopes in arc magmas: Implications for element transfer from the subducted crust. Science, 276(5312): 551-555.

Hein, J.R., Koschinsky, A., Bau, M., Manheim, F.T., Kang, J.-K. and Roberts, L., 2000. Cobalt-rich ferromanganese crusts in the Pacific. In: D.S. Cronan (Editor), Handbook of Marine Mineral Deposits. CRC Press, Boca Raton, pp. 239-280.

Heinrichs, H., Schulz-Dobrick, B. and Wedepohl, K.H., 1980. Terrestrial Geochemistry of Cd, Bi, Tl, Pb, Zn and Rb. Geochim. Cosmochim. Acta., 44: 1519-1533.

Hergt, J.M. and Woodhead, J.D., 2007. A critical evaluation of recent models for Lau-Tonga arc-backarc basin magmatic evolution. Chem. Geol., 245(1-2): 9-44.

Hermann, J. and Green, D.H., 2001. Experimental constraints on high pressure melting in subducted crust. Earth Planet. Sci. Lett., 188(1-2): 149-168.

Hermann, J. and Rubatto, D., 2009. Accessory phase control on the trace element signature of sediment melts in subduction zones. Chem. Geol., 265(3-4): 512-526.

Heydolph, K., Hoernle, K., Hauff, F., van den Bogaard, P., Portnyagin, M., Bindeman, I. and Garbe-Schonberg, D., 2012. Along and across arc geochemical variations in NW Central America: Evidence for involvement of lithospheric pyroxenite. Geochim. Cosmochim. Acta., 84: 459-491.

Hoernle, K., Abt, D.L., Fischer, K.M., Nichols, H., Hauff, F., Abers, G.A., van den Bogaard, P., Heydolph, K., Alvarado, G., Protti, M. and Strauch, W., 2008. Arc-parallel flow in the mantle wedge beneath Costa Rica and Nicaragua. Nature, 451(7182): 1094-U1094.

Jenner, F.E. and O'Neill, H.S.C., 2012. Analysis of 60 elements in 616 ocean floor basaltic glasses. Geochem. Geophys. Geosyst., 13.

Johnson, M.C. and Plank, T., 1999. Dehydration and melting experiments constrain the fate of subducted sediments. Geochem. Geophys. Geosyst., 1.

Kay, R.W., 1978. Aleutian magnesian andesites - melts from subducted Pacific ocean crust. J. Volcanol. Geotherm. Res., 4(1-2): 117-132.

Kay, R.W. and Kay, S.M., 1988. Crustal Recycling and the Aleutian Arc. Geochim. Cosmochim. Acta., 52(6): 1351-1359.

Kay, R.W., Sun, S.S. and Lee-Hu, C.N., 1978. Pb and Sr isotopes in volcanic rocks from the Aleutian Islands and Pribilof Islands, Alaska. Geochim. Cosmochim. Acta., 42(3): 263-273.

Kelemen, P.B., Yogodzinski, G.M. and Scholl, D.W., 2003. Along-strike Variation in Lavas of the Aleutian Island Arc: Implications for the Genesis of High Mg# Andesite and the Continental Crust. Geophysical Monograph, 138: 223-276.

Kelley, K.A., Plank, T., Ludden, J. and Staudigel, H., 2003. Composition of altered oceanic crust at ODP Sites 801 and 1149. Geochem. Geophys. Geosyst., 4.

Kessel, R., Schmidt, M.W., Ulmer, P. and Pettke, T., 2005. Trace element signature of subduction-zone fluids, melts and supercritical liquids at 120-180 km depth. Nature, 437(7059): 724-727.

Leeman, W.P., Carr, M.J. and Morris, J.D., 1994. Boron Geochemistry of the Central-American Volcanic Arc - Constraints on the Genesis of Subduction-Related Magmas. Geochim. Cosmochim. Acta., 58(1): 149-168.

Leeman, W.P., Lewis, J.F., Evarts, R.C., Conrey, R.M. and Streck, M.J., 2005. Petrologic constraints on the thermal structure of the Cascades arc. J. Volcanol. Geotherm. Res., 140(1-3): 67-105.

Marschall, H.R. and Schumacher, J.C., 2012. Arc magmas sourced from melange diapirs in subduction zones. Nature Geoscience, 5(12): 862-867.

Melzer, S. and Wunder, B., 2000. Island-arc basalt alkali ratios: Constraints from phengite-fluid partitioning experiments. Geology, 28(7): 583-586.

Menard, H.W., Natland, J., Jordan, T.H. and Orcutt, J.A., 1983. Site 596: Hydraulic piston coring in an area of low surface productivity in the Southwest Pacific. Initial reports of the deep sea drilling project, 91: 245-267.

Morris, J.D., Leeman, W.P. and Tera, F., 1990. The subducted component in island-arc lavas - constraints from Be isotopes and B-Be systematics. Nature, 344(6261): 31-36.

Nielsen, S.G., Klein, F., Kading, T., Blusztajn, J. and Wickham, K., 2015. Thallium as a Tracer of Fluid-Rock Interaction in the Shallow Mariana Forearc. Earth Planet. Sci. Lett., 430: 416-426.

Nielsen, S.G. and Lee, C.T.A., 2013. Determination of thallium in the USGS glass reference materials BIR-1G, BHVO-2G and BCR-2G and application to quantitative Tl concentrations by LA-ICP-MS. Geostand. Geoanal. Res., 37(3): 337-343.

Nielsen, S.G. and Marschall, H.R., 2017. Geochemical evidence for mélange melting in global arcs. Science Advances, 3: e1602402.

Nielsen, S.G. and Rehkämper, M., 2011. Thallium isotopes and their application to problems in earth and environmental science. In: M. Baskaran (Editor), Handbook of Environmental Isotope Geochemistry. Springer, pp. 247-270.

Nielsen, S.G., Rehkämper, M., Baker, J. and Halliday, A.N., 2004. The precise and accurate determination of thallium isotope compositions and concentrations for water samples by MC-ICPMS. Chem. Geol., 204: 109-124.

Nielsen, S.G., Rehkämper, M., Norman, M.D., Halliday, A.N. and Harrison, D., 2006a. Thallium isotopic evidence for ferromanganese sediments in the mantle source of Hawaiian basalts. Nature, 439: 314-317.

Nielsen, S.G., Rehkämper, M., Porcelli, D., Andersson, P., Halliday, A.N., Swarzenski, P.W., Latkoczy, C. and Gunther, D., 2005. Thallium isotope composition of the upper continental crust and rivers - An investigation of the continental sources of dissolved marine thallium. Geochim. Cosmochim. Acta., 69(8): 2007-2019.

Nielsen, S.G., Rehkämper, M. and Prytulak, J., 2017. Investigation and Application of Thallium Isotope Fractionation. Reviews in Mineralogy and Geochemistry, 82.

Nielsen, S.G., Rehkämper, M., Teagle, D.A.H., Alt, J.C., Butterfield, D. and Halliday, A.N., 2006b. Hydrothermal fluid fluxes calculated from the isotopic mass balance of thallium in the ocean crust. Earth Planet. Sci. Lett., 251(1-2): 120-133.

Nielsen, S.G., Shimizu, N., Lee, C.T.A. and Behn, M., 2014. Chalcophile behavior of thallium during MORB melting and implications for the sulfur content of the mantle. Geochem. Geophys. Geosyst., 15(12): 4905-4919.

Nielsen, S.G., Wasylenki, L.E., Rehkämper, M., Peacock, C.L., Xue, Z. and Moon, E.M., 2013. Towards an understanding of thallium isotope fractionation during adsorption to manganese oxides. Geochim. Cosmochim. Acta., 117: 252-265.

Nielsen, S.G., Yogodzinski, G.M., Prytulak, J., Plank, T., Kay, S.M., Kay, R.W., Blusztajn, J., Owens, J.D., Auro, M. and Kading, T., 2016. Tracking along-arc sediment inputs to the Aleutian arc using thallium isotopes. Geochim. Cosmochim. Acta., 181: 217-237.

Noll, P.D., Newsom, H.E., Leeman, W.P. and Ryan, J.G., 1996. The role of hydrothermal fluids in the production of subduction zone magmas: Evidence from siderophile and chalcophile trace elements and boron. Geochim. Cosmochim. Acta., 60: 587-611.

Patino, L.C., Carr, M.J. and Feigenson, M.D., 1997. Cross-arc geochemical variations in volcanic fields in Honduras CA: progressive changes in source with distance from the volcanic front. Contrib. Mineral. Petrol., 129(4): 341-351.

Patino, L.C., Carr, M.J. and Feigenson, M.D., 2000. Local and regional variations in Central American arc lavas controlled by variations in subducted sediment input. Contrib. Mineral. Petrol., 138(3): 265-283.

Pearce, J.A., Kempton, P.D. and Gill, J.B., 2007. Hf-Nd evidence for the origin and distribution of mantle domains in the SW Pacific. Earth Planet. Sci. Lett., 260(1-2): 98-114.

Plank, T., 2005. Constraints from thorium/lanthanum on sediment recycling at subduction zones and the evolution of the continents. J. Petrol., 46(5): 921-944.

Plank, T. and Langmuir, C.H., 1988. AN EVALUATION OF THE GLOBAL VARIATIONS IN THE MAJOR ELEMENT CHEMISTRY OF ARC BASALTS. Earth Planet. Sci. Lett., 90(4): 349-370.

Plank, T. and Langmuir, C.H., 1993. Tracing trace-elements from sediment input to volcanic output at subduction zones. Nature, 362(6422): 739-743.

Plank, T. and Langmuir, C.H., 1998. The chemical composition of subducting sediment and its consequences for the crust and mantle. Chem. Geol., 145: 325-394.

Prytulak, J., Brett, E.K.A., Webb, M., Rehkämper, M., Plank, T., Savage, P.S. and Woodhead, J., 2016. Thallium elemental behavior and stable isotope fractionation during magmatic processes. Chem. Geol., 345: 139-149.

Prytulak, J., Nielsen, S.G., Plank, T., Barker, M. and Elliott, T., 2013. Assessing the utility of thallium and thallium isotopes for tracing subduction zone inputs to the Mariana arc. Chem. Geol., 345: 139-149.

Reagan, M.K., Morris, J.D., Herrstrom, E.A. and Murrell, M.T., 1994. Uranium Series and Beryllium Isotope Evidence for an Extended History of Subduction Modification of the Mantle Below Nicaragua. Geochim. Cosmochim. Acta., 58(19): 4199-4212.

Regelous, M., Collerson, K.D., Ewart, A. and Wendt, J.I., 1997. Trace element transport rates in subduction zones: evidence from Th, Sr and Pb isotope data for Tonga-Kermadec arc lavas. Earth Planet. Sci. Lett., 150: 291-302.

Regelous, M., Gamble, J.A. and Turner, S.P., 2010. Mechanism and timing of Pb transport from subducted oceanic crust and sediment to the mantle source of arc lavas. Chem. Geol., 273(1-2): 46-54.

Rehkämper, M., Frank, M., Hein, J.R. and Halliday, A., 2004. Cenozoic marine geochemistry of thallium deduced from isotopic studies of ferromanganese crusts and pelagic sediments. Earth Planet. Sci. Lett., 219: 77-91.

Rehkämper, M., Frank, M., Hein, J.R., Porcelli, D., Halliday, A., Ingri, J. and Liebetrau, V., 2002. Thallium isotope variations in seawater and hydrogenetic, diagenetic, and hydrothermal ferromanganese deposits. Earth Planet. Sci. Lett., 197: 65-81.

Rehkämper, M. and Halliday, A.N., 1999. The precise measurement of Tl isotopic compositions by MC- ICPMS: Application to the analysis of geological materials and meteorites. Geochim. Cosmochim. Acta., 63: 935-944.

Rupke, L.H., Morgan, J.P., Hort, M. and Connolly, J.A.D., 2002. Are the regional variations in Central American arc lavas due to differing basaltic versus peridotitic slab sources of fluids? Geology, 30(11): 1035-1038.

Saal, A.E., Kurz, M.D., Hart, S.R., Blusztajn, J.S., Blichert-Toft, J., Liang, Y. and Geist, D.J., 2007. The role of lithospheric gabbros on the composition of Galapagos lavas. Earth Planet. Sci. Lett., 257(3-4): 391-406.

Sadofsky, S.J., Portnyagin, M., Hoernle, K. and van den Bogaard, P., 2008. Subduction cycling of volatiles and trace elements through the Central American volcanic arc: evidence from melt inclusions. Contrib. Mineral. Petrol., 155(4): 433-456.

Salters, V.J.M. and Stracke, A., 2004. Composition of the depleted mantle. Geochem. Geophys. Geosyst., 5.

Schiano, P., Dupré, B. and Lewin, E., 1993. Application of element concentration variability to the study of basalt alteration (Fangataufa atoll, French Polynesia). Chem. Geol., 104(1–4): 99-124.

Schmidt, M.W. and Poli, S., 1998. Experimentally based water budgets for dehydrating slabs and consequences for arc magma generation. Earth Planet. Sci. Lett., 163(1-4): 361-379.

Shannon, R.D., 1976. Revised effective ionic radii and systematic studies of interatomic distances in halides and chalcogenides. Acta Crystallographica, A32: 751-767.

Shaw, D.M., 1952. The geochemistry of thallium. Geochim. Cosmochim. Acta., 2: 118-154.

Shinjo, R., Woodhead, J.D. and Hergt, J.M., 2000. Geochemical variation within the northern Ryukyu Arc: magma source compositions and geodynamic implications. Contrib. Mineral. Petrol., 140: 263-282.

Shu, Y., Nielsen, S.G., Zeng, Z., Shinjo, R. and Blusztajn, J., submitted. Tracing subducted sediment inputs to the Ryukyu arc-Okinawa trough system: Evidence from thallium isotopes. Geochim. Cosmochim. Acta.

Skora, S. and Blundy, J., 2010. High-pressure Hydrous Phase Relations of Radiolarian Clay and Implications for the Involvement of Subducted Sediment in Arc Magmatism. J. Petrol., 51(11): 2211-2243.

Skora, S. and Blundy, J., 2012. Monazite solubility in hydrous silicic melts at high pressure conditions relevant to subduction zone metamorphism. Earth Planet. Sci. Lett., 321: 104-114.

Smith, I.E.M., Brothers, R.N., Muiruri, F.G. and Browne, P.R.L., 1988. The Geochemistry of Rock and Water Samples from Curtis Island Volcano, Kermadec Group, Southwest Pacific. J. Volcanol. Geotherm. Res., 34(3-4): 233-240.

Speeden, I.G., 1973. Site 204. Initial reports of the deep sea drilling project:, 21: 33-56.

Stoiber, R.E. and Carr, M.J., 1973. Quaternary volcanic and tectonic segmentation of Central America. Bulletin Volcanologique, 37(3): 304-325.

Syracuse, E.M., Abers, G.A., Fischer, K., MacKenzie, L., Rychert, C., Protti, M., Gonzalez, V. and Strauch, W., 2008. Seismic tomography and earthquake locations in the Nicaraguan and Costa Rican upper mantle. Geochem. Geophys. Geosyst., 9.

Tera, F., Brown, L., Morris, J., Sacks, I.S., Klein, J. and Middleton, R., 1986. SEDIMENT INCORPORATION IN ISLAND-ARC MAGMAS - INFERENCES FROM BE-10. Geochim. Cosmochim. Acta., 50(4): 535-550.

Turner, S., Caulfield, J., Rushmer, T., Turner, M., Cronin, S., Smith, I. and Handley, H., 2012. Magma Evolution in the Primitive, Intra-oceanic Tonga Arc: Rapid Petrogenesis of Dacites at Fonualei Volcano. J. Petrol., 53(6): 1231-1253.

Turner, S. and Hawkesworth, C., 1997. Constraints on flux rates and mantle dynamics beneath island arcs from Tonga-Kermadec lava geochemistry. Nature, 389(6651): 568-573.

Van Avendonk, H.J.A., Holbrook, W.S., Lizarralde, D. and Denyer, P., 2011. Structure and serpentinization of the subducting Cocos plate offshore Nicaragua and Costa Rica. Geochem. Geophys. Geosyst., 12.

van der Straaten, F., Schenk, V., John, T. and Gao, J., 2008. Blueschist-facies rehydration of eclogites (Tian Shan, NW-China): Implications for fluid–rock interaction in the subduction channel. Chem. Geol., 255(1–2): 195-219.

Vanderkluysen, L., Mahoney, J.J., Koppers, A.A.P., Beier, C., Regelous, M., Gee, J.S. and Lonsdale, P.F., 2014. Louisville Seamount Chain: Petrogenetic processes and geochemical evolution of the mantle source. Geochem. Geophys. Geosyst., 15(6): 2380-2400.

Vogel, T.A., Patino, L.C., Alvarado, G.E. and Gans, P.B., 2004. Silicic ignimbrites within the Costa Rican volcanic front: evidence for the formation of continental crust. Earth Planet. Sci. Lett., 226(1-2): 149-159.

Vogel, T.A., Patino, L.C., Eaton, J.K., Valley, J.W., Rose, W.I., Alvarado, G.E. and Viray, E.L., 2006. Origin of silicic magmas along the Central American volcanic front: Genetic relationship to mafic melts. J. Volcanol. Geotherm. Res., 156(3-4): 217-228.

Walker, J.A., Carr, M.J., Feigenson, M.D. and Kalamarides, R.I., 1990. The Petrogenetic Significance of Interstratified High-Ti and Low-Ti Basalts in Central Nicaragua. J. Petrol., 31(5): 1141-1164.

Walker, J.A., Carr, M.J., Patino, L.C., Johnson, C.M., Feigenson, M.D. and Ward, R.L., 1995. Abrupt Change in Magma Generation Processes across the Central-American Arc in Southeastern Guatemala - Flux Dominated Melting near the Base of the Wedge to Decompression Melting near the Top of the Wedge. Contrib. Mineral. Petrol., 120(3-4): 378-390.

Walker, J.A. and Gazel, E., 2014. Igneous Rock Associations 13. Focusing on the Central American Subduction Zone. Geosci Can, 41: 57-74.

Walker, J.A., Patino, L.C., Cameron, B.I. and Carr, M.J., 2000. Petrogenetic insights provided by compositional transects across the Central American arc: Southeastern Guatemala and Honduras. J. Geophys. Res.-Solid Earth, 105(B8): 18949-18963.

Walker, J.A., Patino, L.C., Carr, M.J. and Feigenson, M.D., 2001. Slab control over HFSE depletions in central Nicaragua. Earth Planet. Sci. Lett., 192(4): 533-543.

Wendt, J.I., Regelous, M., Collerson, K.D. and Ewart, A., 1997. Evidence for a contribution from two mantle plumes to island-arc lavas from northern Tonga. Geology, 25(7): 611-614.

Werner, R., Hoernle, K., Barckhausen, U. and Hauff, F., 2003. Geodynamic evolution of the Galapagos hot spot system (Central East Pacific) over the past 20 m.y.: Constraints from morphology, geochemistry, and magnetic anomalies. Geochem. Geophys. Geosyst., 4.

Woodhead, J.D., Eggins, S.M. and Johnson, R.W., 1998. Magma genesis in the New Britain island arc: Further insights into melting and mass transfer processes. J. Petrol., 39(9): 1641-1668.

Woodhead, J.D. and Johnson, R.W., 1993. Isotopic and Trace-Element Profiles across the New-Britain Island-Arc, Papua-New-Guinea. Contrib. Mineral. Petrol., 113(4): 479-491.

Yogodzinski, G.M., Brown, S.T., Kelemen, P.B., Vervoort, J.D., Portnyagin, M., Sims, K.W.W., Hoernle, K., Jicha, B.R. and Werner, R., 2015. The Role of Subducted Basalt in the Source of Island Arc Magmas: Evidence from Seafloor Lavas of the Western Aleutians. J. Petrol., 56(3): 441-492.

Yogodzinski, G.M., Kay, R.W., Volynets, O.N., Koloskov, A.V. and Kay, S.M., 1995. Magnesian Andesite in the Western Aleutian Komandorsky Region - Implications for Slab Melting and Processes in the Mantle Wedge. Geological Society of America Bulletin, 107(5): 505-519.

Yogodzinski, G.M., Lees, J.M., Churikova, T.G., Dorendorf, F., Woerner, G. and Volynets, O.N., 2001. Geochemical evidence for the melting of subducting oceanic lithosphere at plate edges. Nature, 409(6819): 500-504.

Table 1: Isotope data for Tonga-Kermadec lavas

Sample	Island	Rock type	^{87}Sr/^{86}Sr	^{143}Nd/^{144}Nd	Tl (ng/g)	ε^{205}Tl	n
Tonga							
T068	Tafahi	BA	*0.70390*	0.51293	12.1	2.0	1
T071	Tafahi	B	0.70390	0.51295	5.4	2.2	1
T072	Tafahi	B	*0.70392*	0.51295	10.2	2.2	1
T073	Tafahi	BA	*0.70395*	0.51296	14.2	0.6	1
NT052A	Niuatoputapu	BA	*0.70404*	0.51290	10.3	0.2	1
NT054	Niuatoputapu	BA	*0.70404*	0.51290	23.4	1.4	1
NT059	Niuatoputapu	BA	0.70404	0.51289	21.5	1.3	1
F8	Fonualei	D	*0.70383*	*0.51295*	117	1.1	1
F20	Fonualei	D	*0.70372*	0.51293	117	0.2	1
F30	Fonualei	A	*0.70351*	*0.51297*	100	0.8	1
F31*	Fonualei	A	*0.70392*	*0.51297*	17	-0.6	2
L3*	Late	BA	*0.70367*	*0.51298*	33	7.4	2
L13	Late	BA	*0.70364*	0.51297	144	0.6	1
L20	Late	BA	*0.70355*	0.51298	31.4	1.3	1
L21*	Late	BA	*0.70382*	*0.51297*	42.4	0.6	2
T101P	Kao	BA	*0.70334*	0.51303	32.1	-0.4	1
T102*	Kao	BA	*0.70329*	0.51303	33.8	0.8	2
TOF32*	Tofua	A	*0.70350*	*0.51302*	46.3	3.7	2
HHBF	Hunga Ha'apai	BA	*0.70376*	*0.51296*	106	-0.2	1
38983	Hunga Tonga	BA	*0.70365*	0.51299	47.7	0.2	1
Kermadec							
14782	Raoul Group	B	*0.70360*	*0.51300*	6.4	0.4	1
23374	Raoul Group	BA	*0.70347*	0.51305	21.3	0.7	1
23383*	Raoul Group	BA	*0.70376*	0.51302	12.5	2.0	1
23386*	Raoul Group	A	*0.70355*	0.51305	11.3	2.4	2
10379	Macauley	B	*0.70347*	*0.51301*	15.6	4.7	2
10380	Macauley	B	*0.70350*	0.51300	11.7	4.3	2
14849	Curtis	BA	*0.70410*	*0.51301*	39.2	-0.5	1
14864	Curtis	D	*0.70408*	*0.51301*	75.4	-0.1	1
14831	L'Esperance	BA		0.51297	22.4	5.3	2
14837*	L'Esperance	BA	*0.70402*	*0.51297*	21.3	12.3	2

Numbers in italics denote data from (Ewart et al., 1998; Regelous et al., 1997; Regelous et al., 2010). B - basalt; BA - basaltic andesite; A - andesite; D - dacite

* - samples that were received as chips (see text for description of sample processing)

n - number of total procedural repeats (dissolution, chemical separation, mass spectrometry)

Table 2: Major element data for Tonga-Kermadec lavas in wt%

	SiO_2	TiO_2	Al_2O_3	Fe_2O_3	MnO	MgO	CaO	Na_2O	K_2O	P_2O_5	LOI	SUM
T068 Tafahi	52.52	0.360	16.83	11.16	0.195	6.62	11.52	0.358	0.185	0.117	≤0.01	99.86
T071 Tafahi	51.53	0.355	17.52	10.85	0.189	6.65	12.21	0.312	0.163	0.091	≤0.01	99.87
T072 Tafahi	51.85	0.347	17.00	10.70	0.191	6.93	12.26	0.312	0.172	0.092	≤0.01	99.85
T073 Tafahi	52.51	0.435	16.96	11.57	0.198	5.81	11.46	0.594	0.186	0.107	≤0.01	99.82
T052a Niuatoputapu	54.57	0.412	15.58	12.50	0.204	4.73	10.47	0.858	0.363	0.132	≤0.01	99.82
T054 Niuatoputapu	54.18	0.305	15.39	10.46	0.192	7.10	11.30	0.316	0.321	0.105	0.17	99.84
T059 Niuatoputapu	54.13	0.303	15.22	10.83	0.192	7.23	11.10	0.347	0.321	0.109	0.05	99.83
FON-8 Fonualei	65.22	0.579	13.37	8.58	0.191	1.56	5.78	3.20	1.13	0.262	≤0.01	99.87
FON-20 Fonualei	65.03	0.545	13.86	8.55	0.182	1.52	5.79	3.09	1.10	0.209	≤0.01	99.87
FON-30 Fonualei	60.28	0.633	14.40	10.95	0.204	2.60	7.42	2.34	0.846	0.191	≤0.01	99.86
FON-31 Fonualei	60.33	0.629	14.21	11.03	0.208	2.61	7.39	2.42	0.803	0.226	≤0.01	99.86
Late 3	54.31	0.587	15.78	11.41	0.197	5.17	10.38	1.30	0.518	0.178	≤0.01	99.83
Late 13	57.09	0.778	14.20	13.00	0.213	3.26	8.22	2.20	0.664	0.186	≤0.01	99.81
Late 20	53.58	0.518	16.21	10.90	0.192	5.82	11.14	0.958	0.413	0.118	≤0.01	99.84
Late 21	53.47	0.578	16.51	11.56	0.196	4.85	10.83	1.22	0.456	0.154	≤0.01	99.82
T101P Kao	52.77	0.805	17.46	10.95	0.171	4.28	10.81	1.82	0.542	0.233	≤0.01	99.84
T102 Kao	53.39	0.766	16.29	11.36	0.188	5.37	10.06	1.72	0.488	0.189	≤0.01	99.83
TOF-32 Tofua	57.07	0.714	14.66	11.46	0.200	4.04	9.01	1.88	0.597	0.208	≤0.01	99.84
HHBF Hunga Ha'apai	54.54	0.492	17.79	9.74	0.167	4.23	11.34	1.09	0.338	0.123	≤0.01	99.85
38983 Hunga Tonga	55.70	0.578	14.87	11.28	0.196	5.05	10.26	1.29	0.435	0.160	≤0.01	99.82
14782 Raoul	48.90	0.722	16.01	11.98	0.201	7.36	12.07	1.93	0.117	0.143	0.41	99.83
23374 Raoul	52.28	0.599	15.76	9.87	0.192	7.16	11.79	1.84	0.252	0.128	≤0.01	99.87
23383 Raoul	53.03	0.646	17.29	10.40	0.178	5.14	10.72	2.12	0.200	0.105	0.05	99.87
23386 Raoul	56.38	0.703	17.51	9.05	0.179	3.34	9.79	2.54	0.260	0.143	≤0.01	99.89
10379 Macauley	48.01	0.619	19.73	9.75	0.174	5.80	13.33	1.91	0.382	0.149	≤0.01	99.85
10380 Macauley	48.56	0.861	14.89	13.40	0.229	7.05	12.07	2.11	0.454	0.170	≤0.01	99.79
14849 Curtis	52.46	0.503	15.52	11.02	0.188	5.76	10.97	1.77	0.403	0.124	1.13	99.85
14864 Curtis	65.55	0.542	14.73	5.49	0.142	1.70	5.47	3.59	1.20	0.182	1.29	99.88
14831 L Esperance	52.86	1.02	16.56	13.54	0.258	4.62	9.59	0.341	0.220	0.547	0.24	99.79
14837 L Esperance	51.67	0.982	16.39	13.44	0.238	4.984	10.11	1.506	0.360	0.172	≤0.01	99.85

LOI - loss on ignition

Table 3: Thallium isotope compositions and concentrations for Tonga-Kermadec sediments

Site	Core	Section	Interval (cm)	Depth (m)	Tl (ng/g)	$\varepsilon^{205}Tl$
Pelagic sediments						
204	1	1	30-33	0.3	834	1.0
204	1	3	52-55	3.52	681	1.5
204	5	5	60–63	100.6	2929	4.5
596	1	1	115–118	1.15	1556	3.6
596	2	3	85–88	9.35	1254	2.3
596	2	6	77–80	13.77	3067	6.6
596	3	6	84–87	23.44	3746	2.3
596	6	6	124–127	48.54	940	1.1
Average					**1876**	**3.6**
Volcaniclastic sediments						
204	1	4	103–106	5.53	328	0.0
204	3	2	103–106	50.53	151	-0.7
204	6	2	66–69	105.16	184	1.6
204	9	3	67–70	144.67	192	0.7
Average					**214**	**0.4**

Table 4: Thallium isotope compositions and concentrations for Central American lavas and sediments

Sample	Volcano	Tl (ng/g)	ε^{205}Tl	n
lavas				
CR-IZ-63A	Irazu	81	-1.4	2
CR-IZ-D6	Irazu	243	-8.2	2
CR-B2	Barba	39	-2.0	2
CR-PO10	Sabana Redonda	76	-3.8	1
CR-PP6	Platanar	91	-2.5	2
CR-124 (LA)	Arenal	15	-0.8	1
CR-123 (LA)	Arenal	16	-1.9	4
CR-TE9	Tenorio	36	-3.6	1
NIC-GR5	Granada	5.8	3.5	1
NIC-GR3	Granada	34	4.7	1
NIC-MS7	Masaya	29	-1.2	4
NIC-NE201	Nejapa	4.5	9.0	1
NIC-NE202	Nejapa	8.7	-11.5	3
NIC-NE5	Nejapa	14	1.0	1
NIC-NE203	Nejapa	nd	0.1	1
NIC-CN10	Cerro Negro	46	-0.1	2
NIC-TE1	Telica	92	-1.1	1
NIC-TE6	Telica	48	-1.8	1
NIC-TE123	Telica	75	-2.0	2
NIC-SC2	San Cristobal	34	-1.9	2
NIC-COS9A	Cosiguina	78	-1.8	2
SAL-CON-3	Conchagua	40	-3.1	2
SAL-SM-7	San Miguel	46	-1.6	2
SAL-AP-3	Apastapeque	134	-4.6	2
SAL-B-21	Boqueron	145	-1.4	2
SAL-IZ108	Izalco	59	2.0	2
SAL-CV1	Cerro Verde	60	-1.7	2
GU-T302	Tecuamburro	40	-1.3	2
GU-C201	C. Mongoy	51	-2.5	1
GU-C303	C. del Cemeterio	26	0.9	1
GU-E1	Pacaya	61	1.1	2
GU-C837	Cerro Las Olivas	71	-1.6	1
GU-74-27 (VF)	Fuego	35	-0.1	2
GU-SM126	Santa Maria	42	-1.3	2
sediments, DSDP 495				
41-43	hemipelagic	1077	0.2	1
111-113	carbonate	33	5.8	1

n - number of isotopic measurements

nd - not determined

Major and trace elements and isotope ratios for these samples can be found in (Carr et al., 2014)

1238

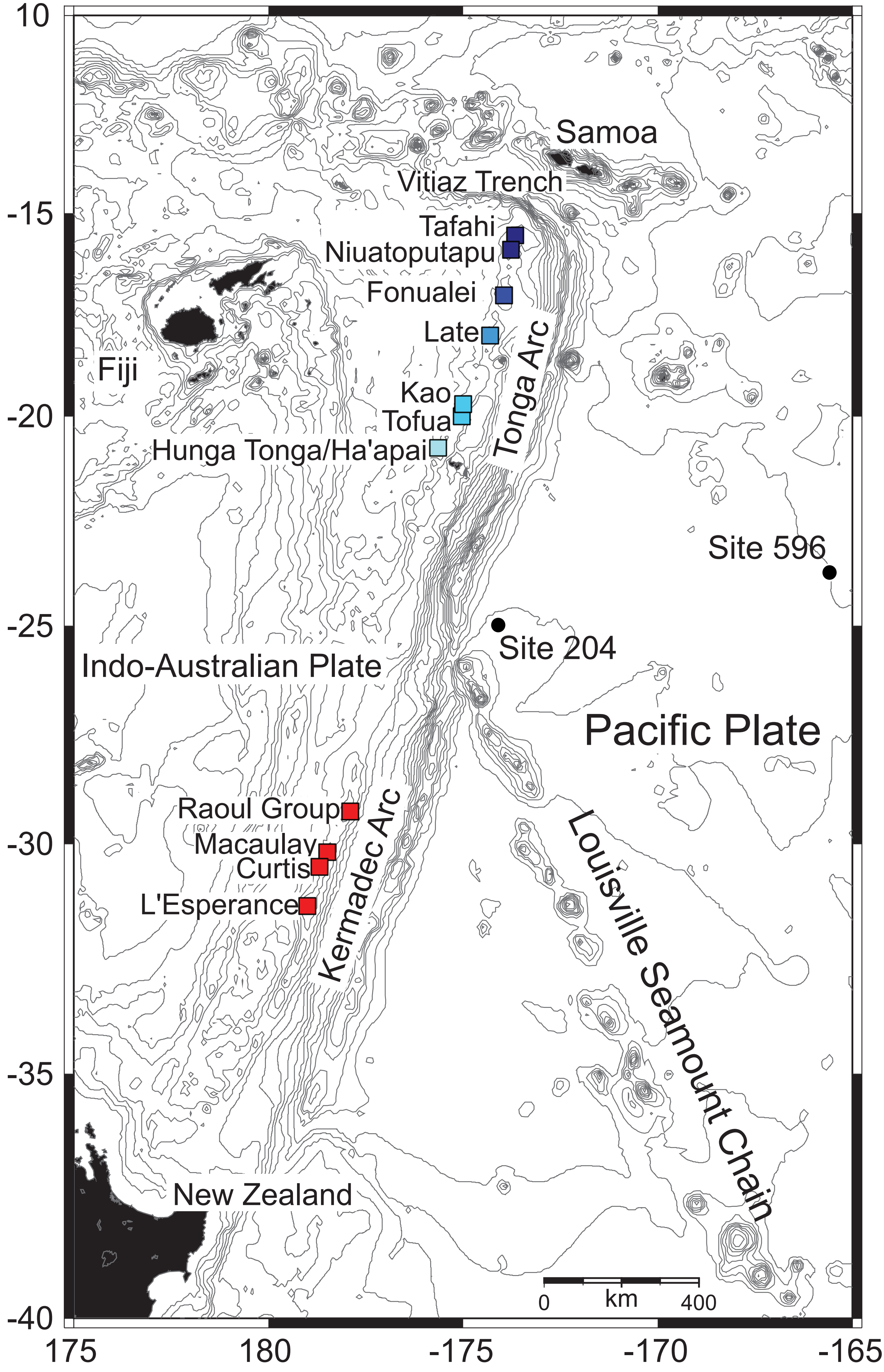

Samoa
Vitiaz Trench
Tafahi
Niuatoputapu
Fonualei
Late
Fiji
Kao
Tofua
Tonga Arc
Hunga Tonga/Ha'apai
Site 596
Site 204
Indo-Australian Plate
Pacific Plate
Raoul Group
Macaulay
Curtis
L'Esperance
Kermadec Arc
Louisville Seamount Chain
New Zealand
0
km
400
10
-15
-20
-25
-30
-35
-40
175
180
-175
-170
-165

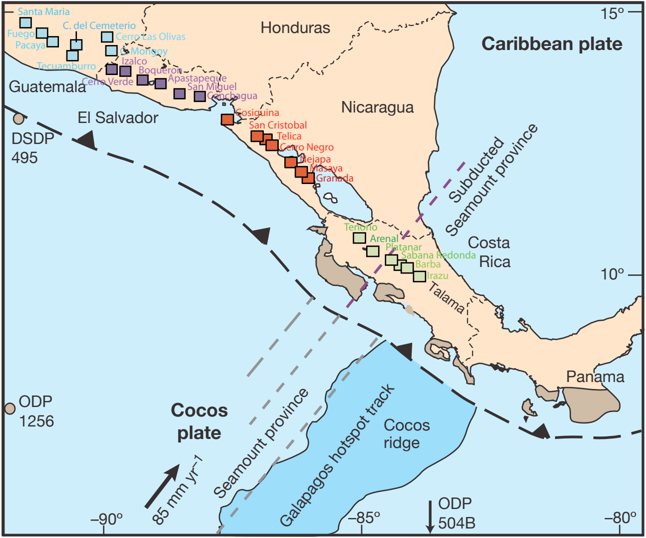

Santa Maria
Fuego
Pacaya
C. del Cemeterio
Cerro Las Olivas
C. Mongoy
Tecuamburro
Izalco
Boqueron
Cerro Verde
Apastapeque
San Miguel
Conchagua
Cosiguina
San Cristobal
Telica
Cerro Negro
Nejapa
Masaya
Granada
Tenorio
Arenal
Platanar
Sabana Redonda
Barba
Irazu
Honduras
Guatemala
El Salvador
Nicaragua
Costa Rica
Panama
Talama
Caribbean plate
Cocos plate
Cocos ridge
Subducted Seamount province
Seamount province
Galapagos hotspot track
DSDP 495
ODP 1256
ODP 504B
85 mm yr−1
15°
10°
−90°
−85°
−80°

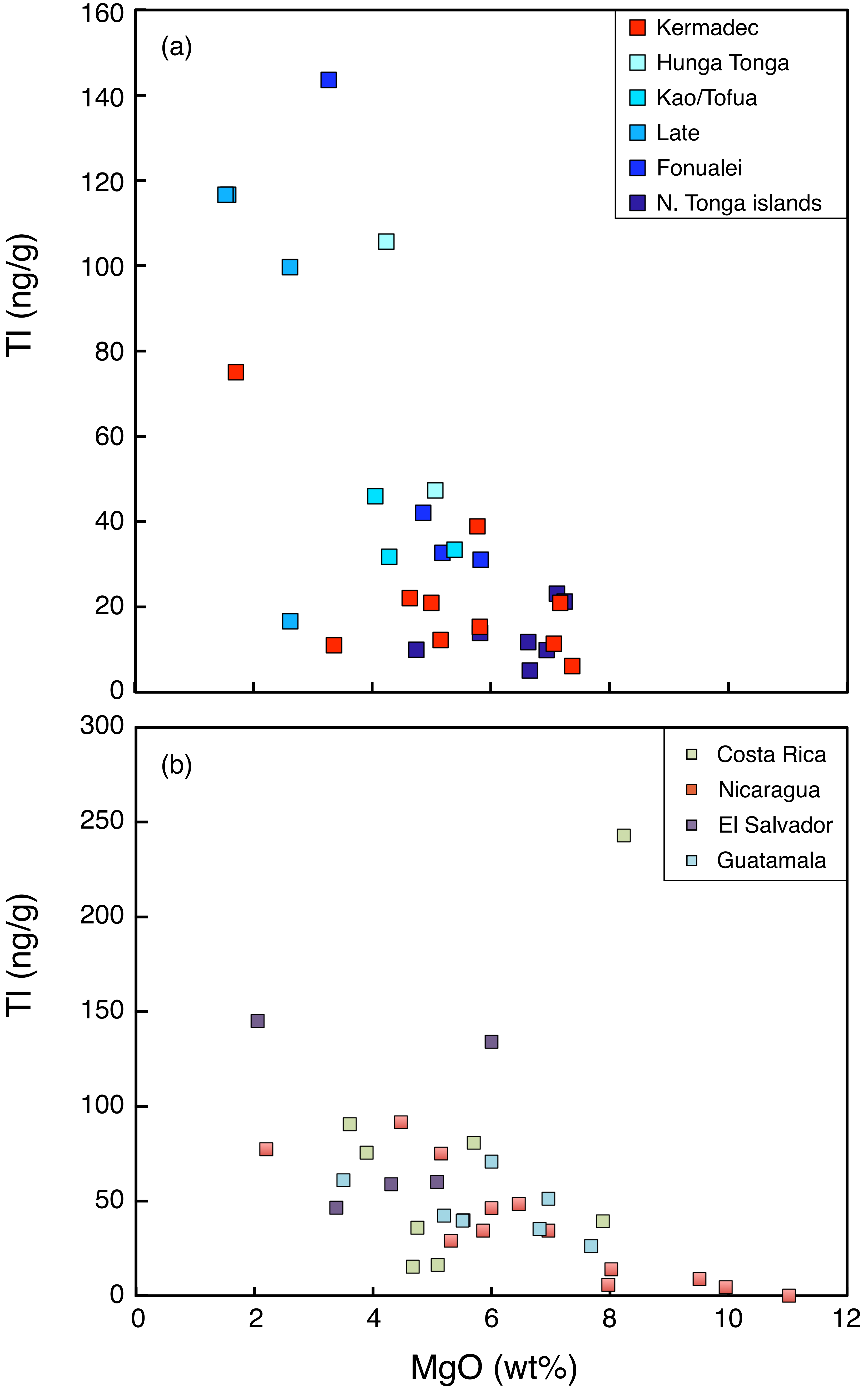

(a)
Kermadec
Hunga Tonga
Kao/Tofua
Late
Fonualei
N. Tonga islands
Tl (ng/g)
0
20
40
60
80
100
120
140
160
(b)
Costa Rica
Nicaragua
El Salvador
Guatamala
Tl (ng/g)
0
50
100
150
200
250
300
0
2
4
6
8
10
12
MgO (wt%)

(a)
altered Hawaiian lava
subaerial weathering - Tl and Rb loss
altered Aleutian lava
Ce/Tl
Th/Rb
(b)
Costa Rica
Nicaragua
El Salvador
Guatamala
NE-201
GR-5
NE-202
DMM
Irazu
Unaltered Aleutian lavas
(c)
Kermadec
Hunga Tonga
Kao/Tofua
Late
Fonualei
N. Tonga islands
Macaulay 10380

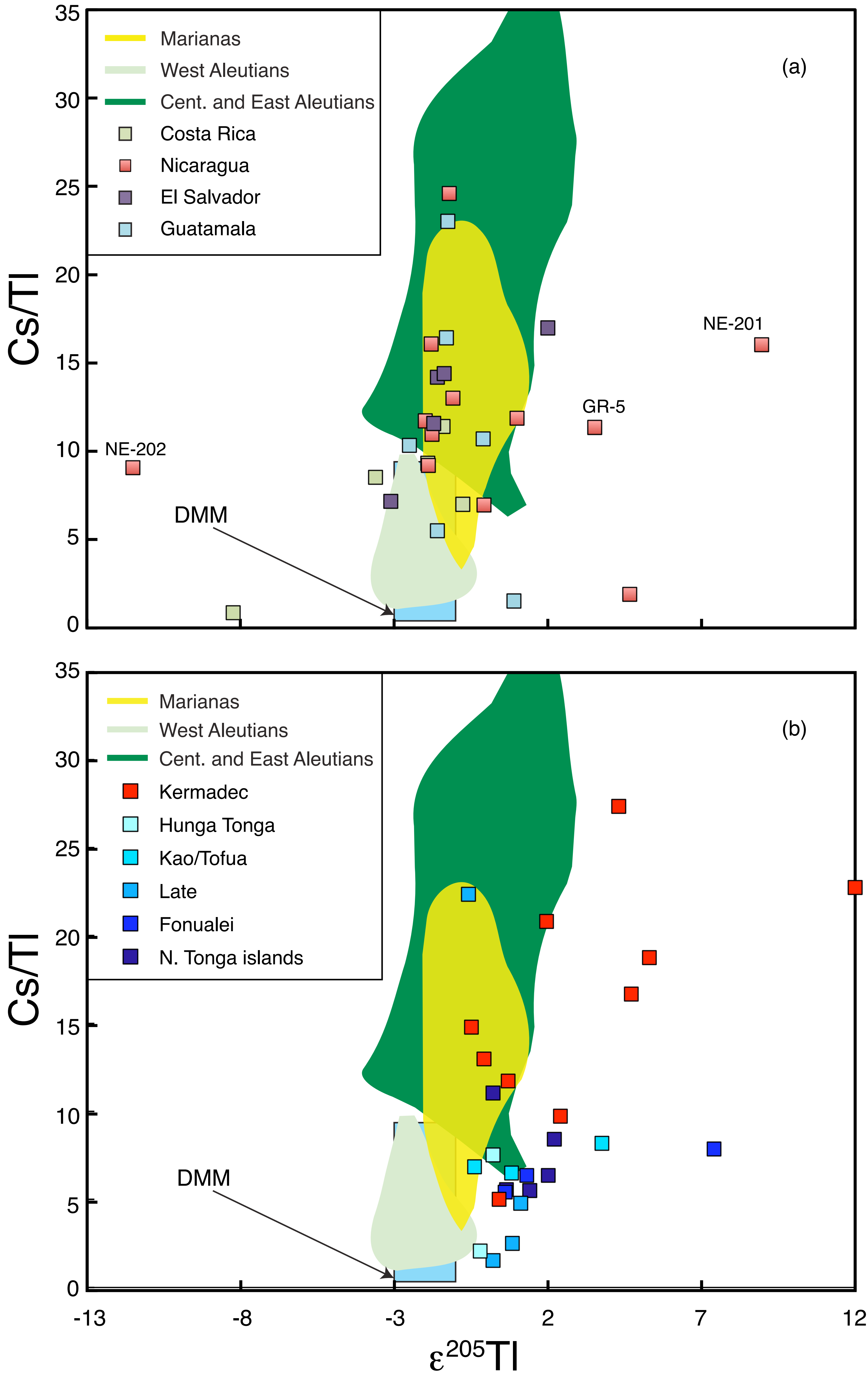

Marianas
West Aleutians
Cent. and East Aleutians
Costa Rica
Nicaragua
El Salvador
Guatamala
(a)
NE-201
GR-5
NE-202
DMM
Cs/Tl
Marianas
West Aleutians
Cent. and East Aleutians
Kermadec
Hunga Tonga
Kao/Tofua
Late
Fonualei
N. Tonga islands
(b)
DMM
Cs/Tl
0
5
10
15
20
25
30
35
-13
-8
-3
2
7
12
$\varepsilon^{205}Tl$

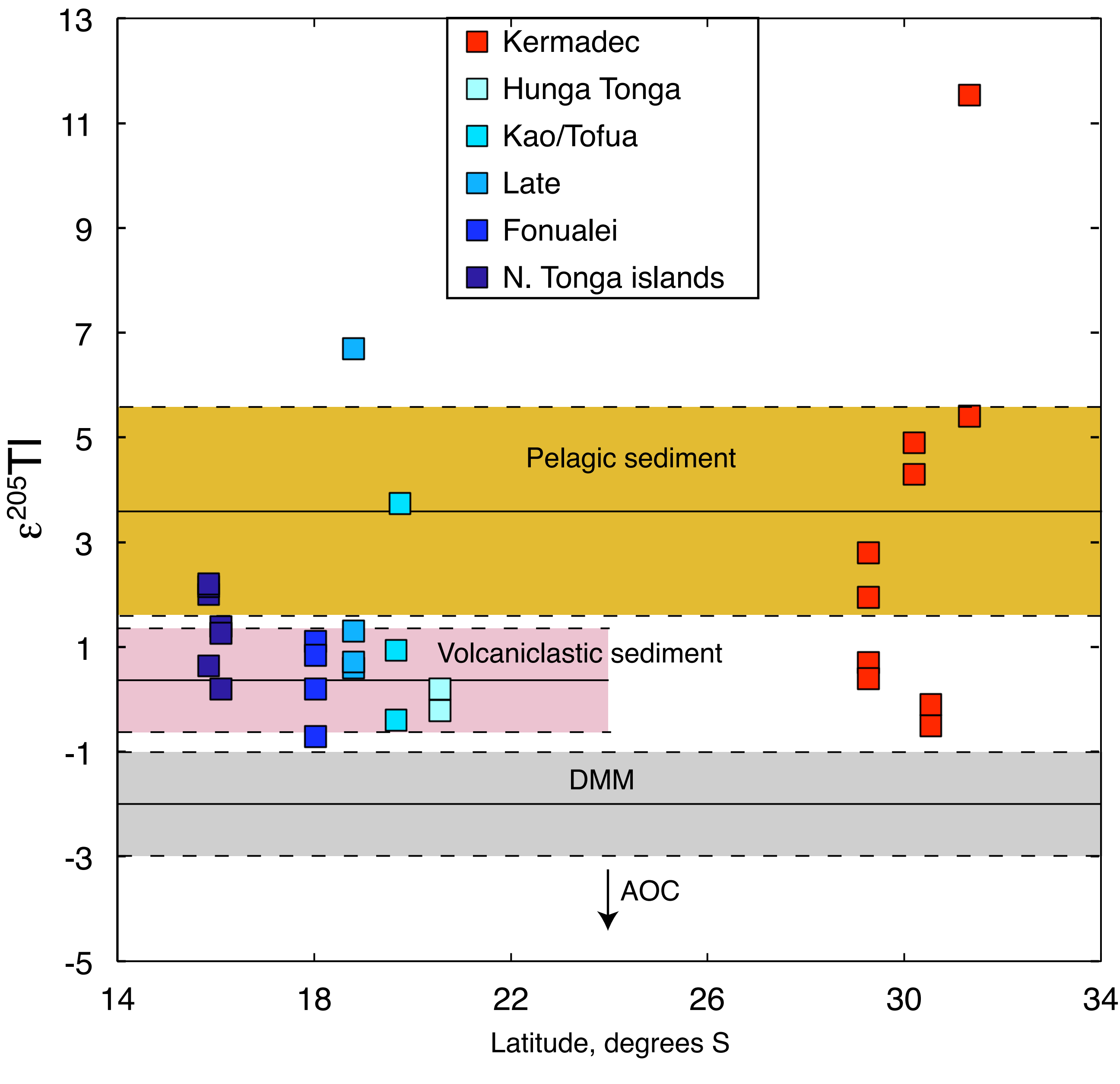
Kermadec
Hunga Tonga
Kao/Tofua
Late
Fonualei
N. Tonga islands
Pelagic sediment
Volcaniclastic sediment
DMM
AOC
ε^{205}Tl
Latitude, degrees S
13
11
9
7
5
3
1
-1
-3
-5
14
18
22
26
30
34

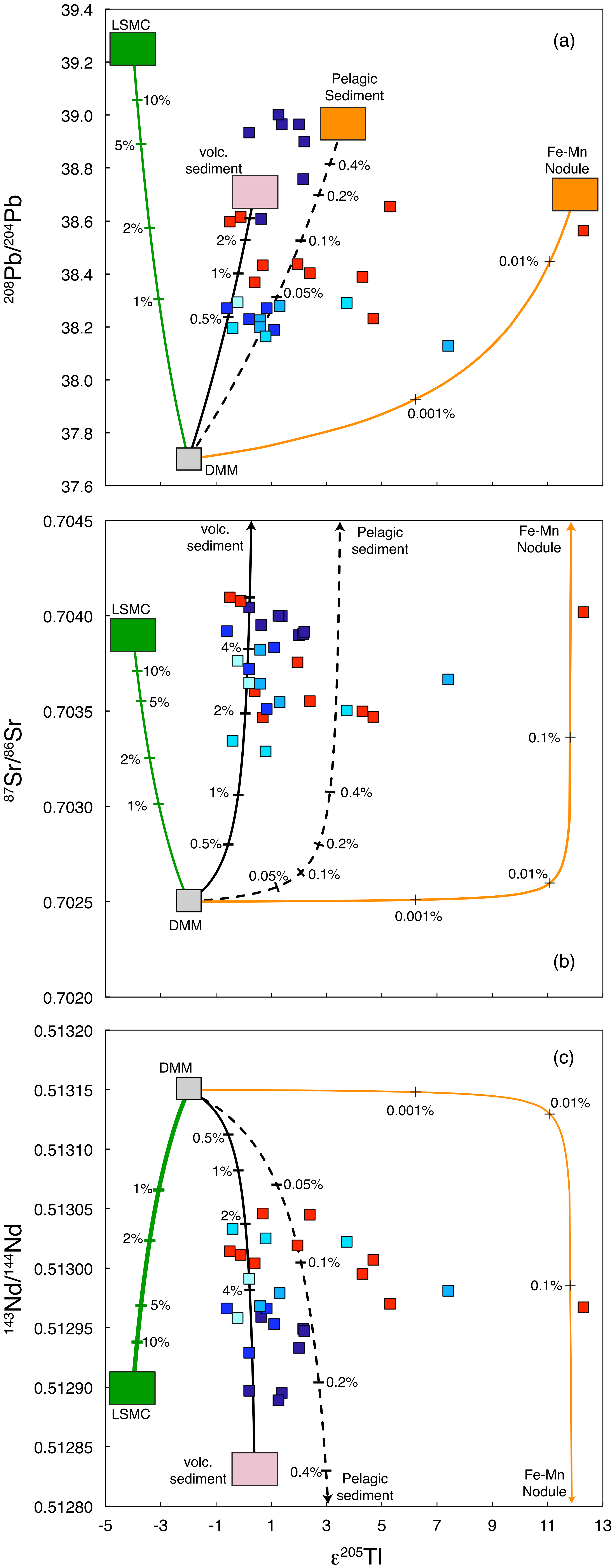

(a)
LSMC
Pelagic Sediment
volc. sediment
Fe-Mn Nodule
DMM
10%
5%
2%
1%
0.5%
0.4%
0.2%
0.1%
0.05%
0.01%
0.001%
$^{208}Pb/^{204}Pb$
39.4
39.2
39.0
38.8
38.6
38.4
38.2
38.0
37.8
37.6
(b)
volc. sediment
Pelagic sediment
Fe-Mn Nodule
LSMC
DMM
4%
2%
1%
0.5%
0.4%
0.2%
0.1%
0.05%
0.01%
0.001%
$^{87}Sr/^{86}Sr$
0.7045
0.7040
0.7035
0.7030
0.7025
0.7020
(c)
DMM
LSMC
volc. sediment
Pelagic sediment
Fe-Mn Nodule
0.5%
1%
2%
4%
5%
10%
0.05%
0.1%
0.2%
0.4%
0.001%
0.01%
$^{143}Nd/^{144}Nd$
0.51320
0.51315
0.51310
0.51305
0.51300
0.51295
0.51290
0.51285
0.51280
-5
-3
-1
1
3
5
7
9
11
13
$\varepsilon^{205}Tl$

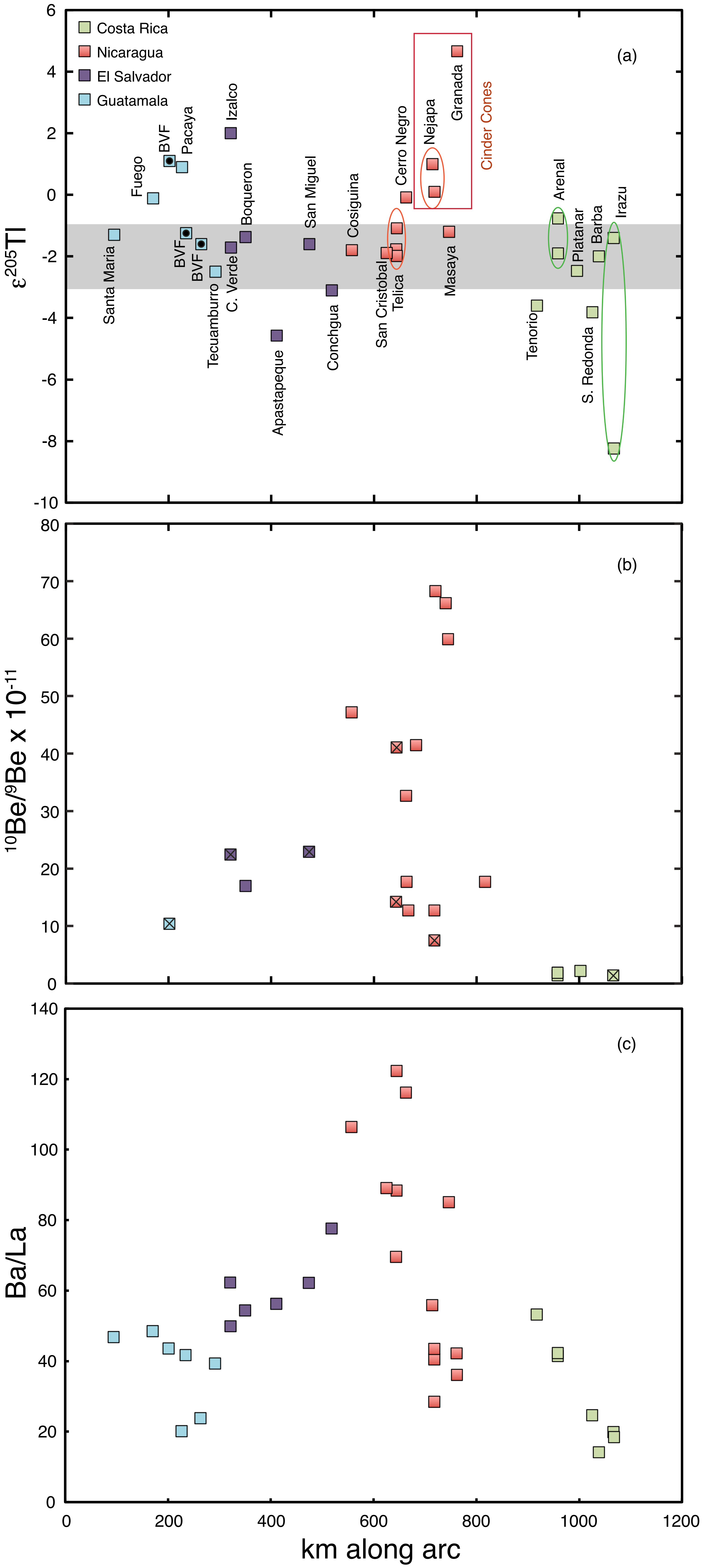

Costa Rica
Nicaragua
El Salvador
Guatamala
(a)
Cinder Cones
Santa Maria
Fuego
BVF
Pacaya
Izalco
BVF
BVF
Tecuamburro
C. Verde
Boqueron
Apastapeque
San Miguel
Conchgua
Cosiguina
San Cristobal
Telica
Cerro Negro
Nejapa
Granada
Masaya
Tenorio
Arenal
Platanar
S. Redonda
Barba
Irazu
ε^{205}Tl
(b)
^{10}Be/^{9}Be x 10^{-11}
(c)
Ba/La
km along arc

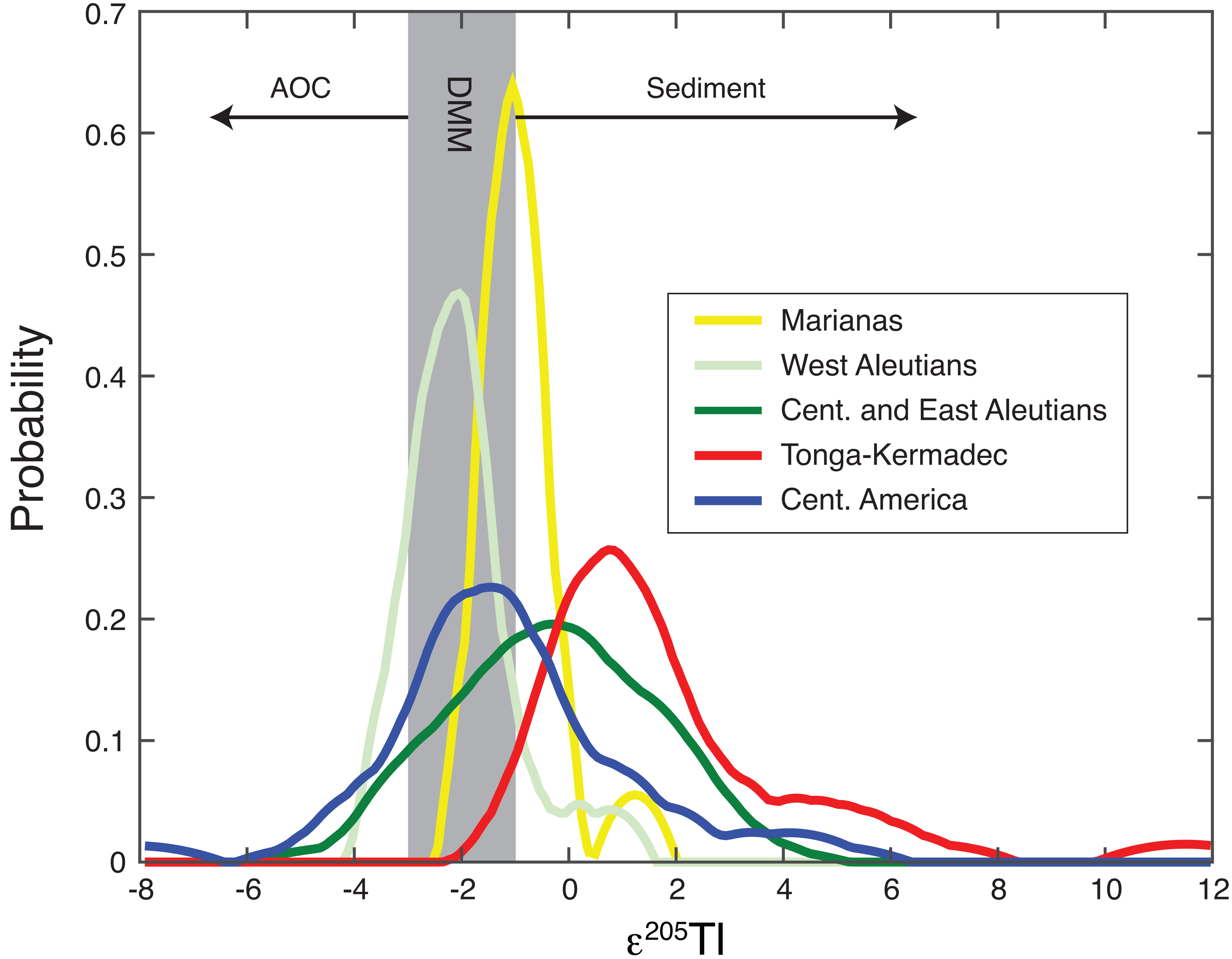

AOC
DMM
Sediment
Marianas
West Aleutians
Cent. and East Aleutians
Tonga-Kermadec
Cent. America
Probability
0.7
0.6
0.5
0.4
0.3
0.2
0.1
0
-8
-6
-4
-2
0
2
4
6
8
10
12
$\varepsilon^{205}Tl$

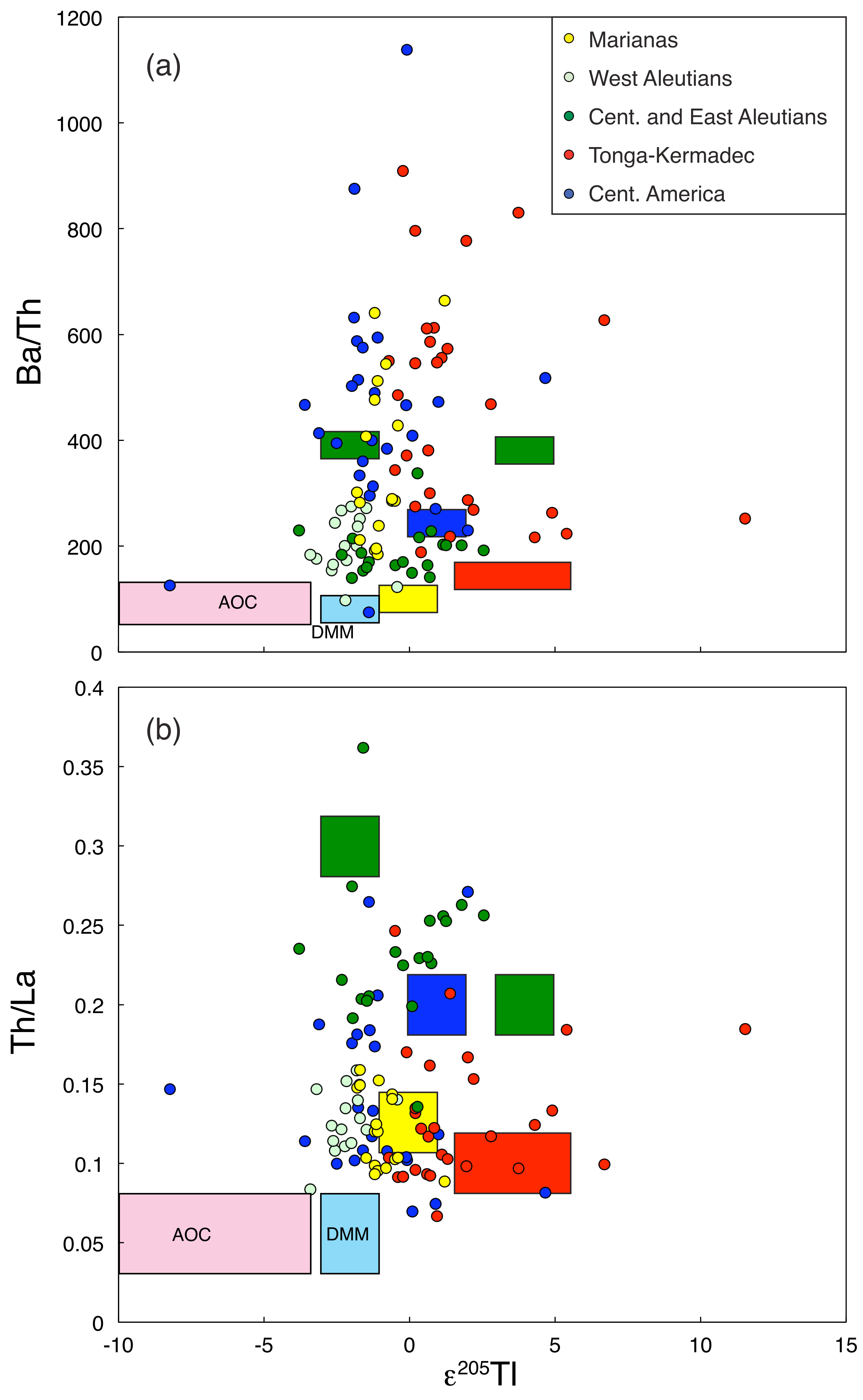

(a)
Marianas
West Aleutians
Cent. and East Aleutians
Tonga-Kermadec
Cent. America
Ba/Th
1200
1000
800
600
400
200
0
AOC
DMM
(b)
Th/La
0.4
0.35
0.3
0.25
0.2
0.15
0.1
0.05
0
AOC
DMM
-10
-5
0
5
10
15
ε205Tl

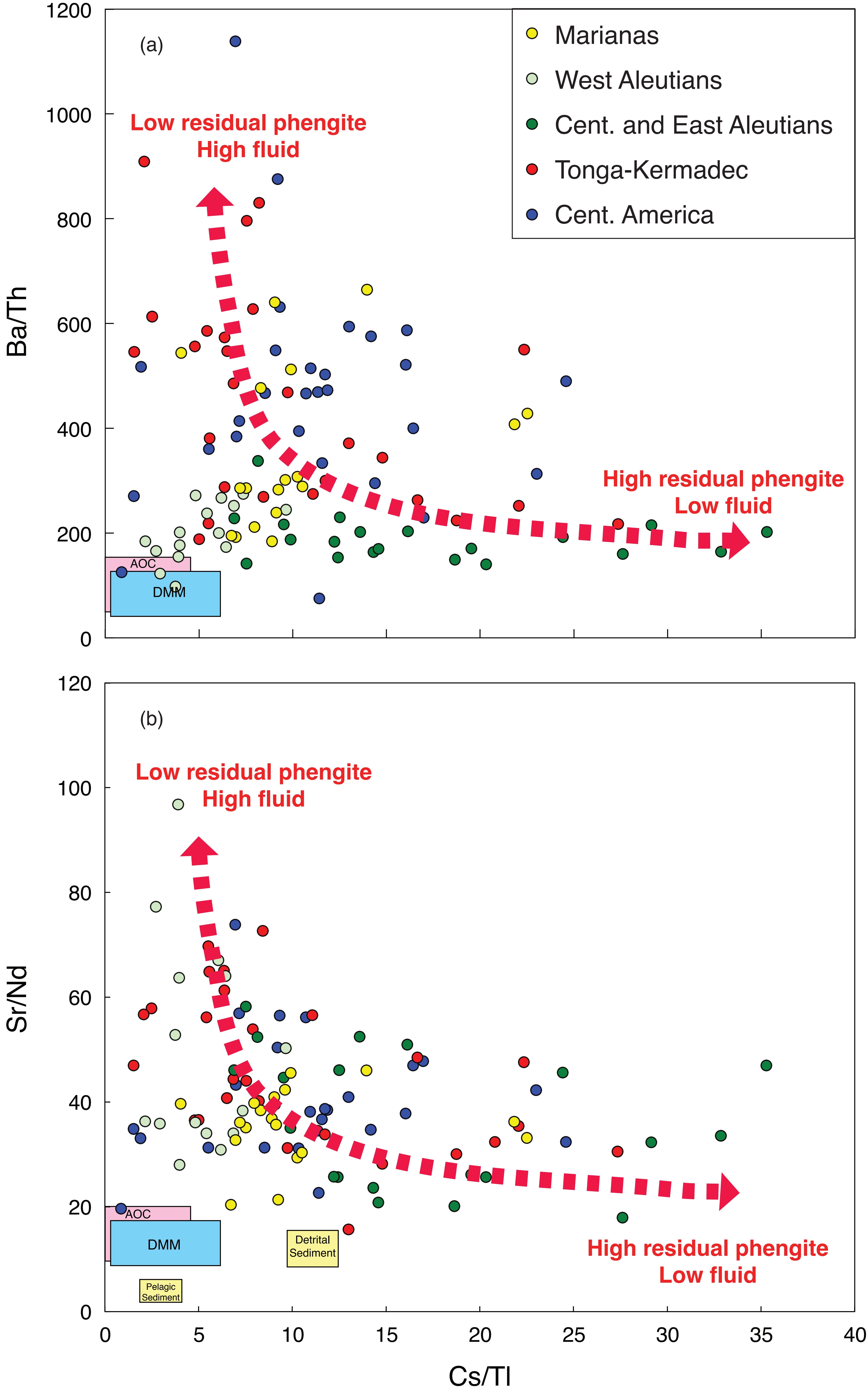

(a)
Marianas
West Aleutians
Cent. and East Aleutians
Tonga-Kermadec
Cent. America
Low residual phengite
High fluid
High residual phengite
Low fluid
AOC
DMM
Ba/Th
0
200
400
600
800
1000
1200
(b)
Low residual phengite
High fluid
High residual phengite
Low fluid
AOC
DMM
Detrital Sediment
Pelagic Sediment
Sr/Nd
0
20
40
60
80
100
120
0
5
10
15
20
25
30
35
40
Cs/Tl

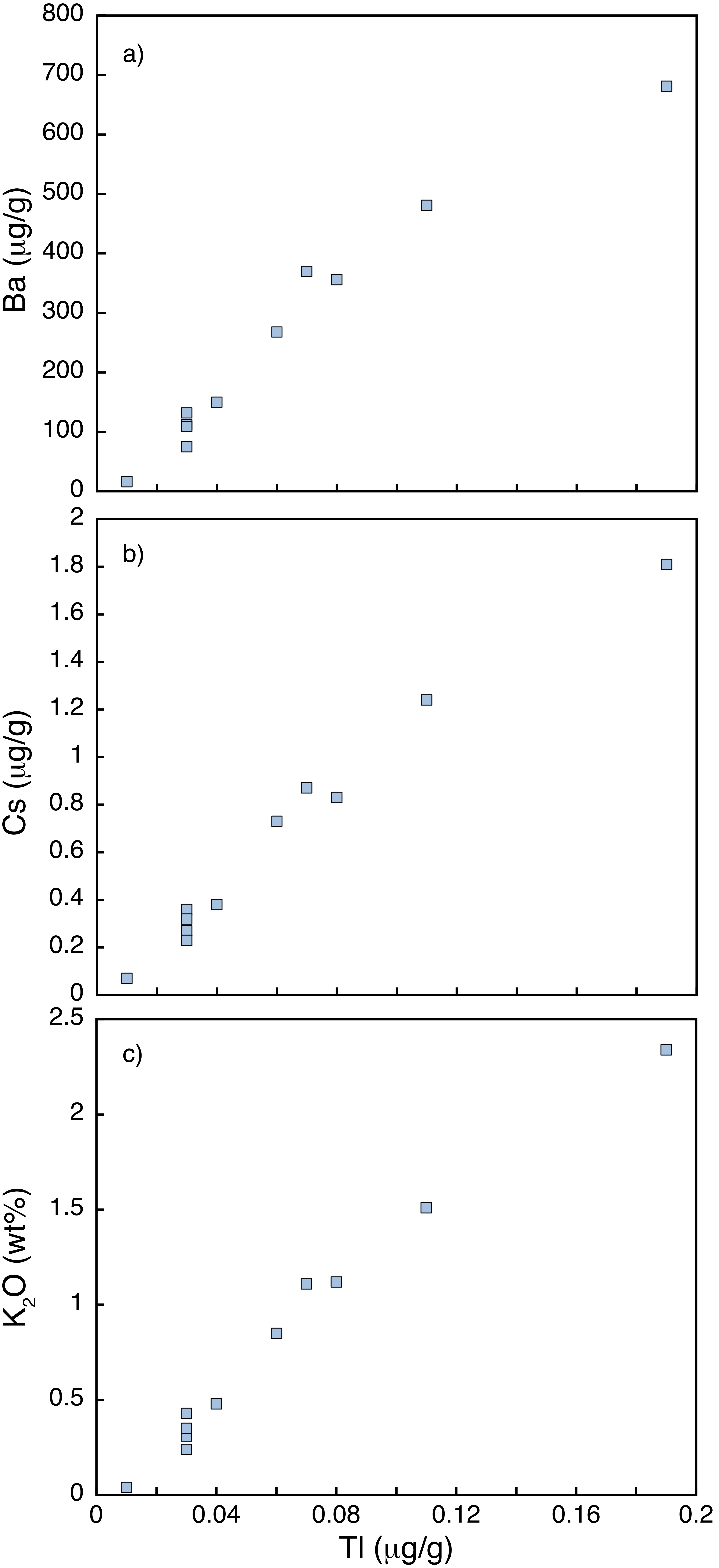

a)
Ba (μg/g)
0
100
200
300
400
500
600
700
800
b)
Cs (μg/g)
0
0.2
0.4
0.6
0.8
1
1.2
1.4
1.6
1.8
2
c)
K2O (wt%)
0
0.5
1
1.5
2
2.5
0
0.04
0.08
0.12
0.16
0.2
Tl (μg/g)